DOI: 10.1002/(( ))
Article type: Communication

Over 20% PCE perovskite solar cells with superior stability achieved by novel and low-cost hole-transporting materials

Fei Zhang ,Zhiqiang Wang, Hongwei Zhu, Norman Pellet,Jingshan Luo, Chenyi Yi, Xicheng Liu,Shirong Wang, Xianggao Li , Yin Xiao, Shaik Mohammed Zakeeruddin* , Dongqin Bi*, Michael Grätzel**

F. Zhang, Z.Wang,H.Zhu,Dr.Y.Xiao, Prof. S. Wang ,Prof. X. Li, *
School of Chemical Engineering and Technology, Tianjin University
300072 Tianjin, China
Email: lixianggao@tju.edu.cn

F. Zhang, N.Pellet, Dr. J. Luo, Dr. C. Yi, Dr. S. M. Zakeeruddin, Dr. D. Bi , Prof. M. Grätzel*
Laboratory of Photonics and Interfaces, Institute of Chemical Sciences and Engineering,
École Polytechnique Fédérale de Lausanne (EPFL)
Station 6 CH-1015, Lausanne, Switzerland
Email: shaik.zakeer@epfl.ch ; dongqin.bi@epfl.ch ; michael.graetzel@epfl.ch

F. Zhang, Z.Wang,H.Zhu,Dr.Y.Xiao, Prof. S. Wang ,Prof. X. Li, *
Collaborative Innovation Center of Chemical Science and Engineering(Tianjin)
300072 Tianjin, China

Dr.X.Liu
Qufu Normal University, School of Chemistry and Chemical Engineering,
273165 Qufu, China

N.Pellet
Max Planck Institute for Solid State Research
Heisenbergstrasse 1, Stuttgart 70569, Germany

Keywords: stability; thiophene; hole transporting materials; perovskite solar cell

Abstract: The exploration of alternative low-cost molecular hole-transporting materials (HTMs) specifically for both high efficient and stable perovskite solar cells (PSCs) is a relatively new research area. Two novel HTMs using the thiophene core were designed and synthesized (Z25 and Z26). The Z26-based perovskite solar cells exhibited a remarkable overall power conversion efficiency (PCE) of 20.1 %, which is comparable to 20.6% obtained by spiro-OMeTAD-based device. Importantly, the devices based-on Z26 show better stability

compared to devices based on Z25 and spiro-OMeTAD when aged under ambient air of 30% or 85% relative humidity in the dark and under continuous full sun illumination at maximum power point tracking respectively. The presented results clearly qualify a simple strategy by introduction of double bonds to design hole transporting materials for highly efficient and stable perovskite solar cells with lower cost, which is important for the future development of materials for commercial application.

In recent years, perovskite-based solar cells (PSCs) have attracted great attention in photovoltaics due to three significant advantages: inexpensive precursors, simple fabrication methods, and remarkably high power conversion efficiency (PCE) values.[1-3] Typical PSC configuration is composed of perovskite absorbing material sandwiched between an electron transporting material (ETM) and a hole transporting material (HTM), the latter playing an important role to facilitate the transportation of holes from the perovskite to back contact.[4]

Spiro-based organic semiconductor 2,2',7,7'-tetrakis-(N,N'-di-4-methoxyphenylamine)-9,9'-spirobifluorene (spiro-OMeTAD) was selected as the benchmark HTM for PSC.[5,6] However, the tedious multi-step synthesis of spiro-OMeTAD makes it prohibitively expensive and cost-ineffective. Typically, high-purity sublimation-grade spiro-OMeTAD is required to obtain high-performance devices.[7] The development of novel small-molecule organic semiconductors has to find a better understanding between HTM structure and PSC performance.[7-29] However, new HTMs that can really replace spiro-OMeTAD in terms of high device efficiency are scarce. Care must also be taken since HTMs may show different hysteresis behavior depending on their structure. Due to charge accumulation at interfaces or dielectric polarization of the perovskite layer,[30,31] photocurrent density-voltage (J-V) hysteresis with respect to the scan direction can lead to overestimation of the PCE. [32,33]

Therefore, in order to make a fair evaluation of new HTMs, high efficient perovskite solar cells with good reproducibility,high stability and low cost should be employed.

Thiophenes represent an class of building blocks for organic semiconductor materials, and were widely investigated owing to their favorable optoelectronic properties and in particularly their high hole mobility presenting an attractive feature for HTM design.[34] Moreover, thiophene–iodine interaction can promote photogenerated hole transporting.[25] However, apart from a few exceptions, [25,29] most PSCs based on thiophene HTMs show a PCE lower than 16%.[35-42]

Herein, we report the synthesis and characterization as well as the application in perovskite solar cells of two novel thiophene-based HTMs, coded Z25 and Z26. The latter is derived by introdution of two double bonds into Z25 as shown in **Figure 1a**. Devices, fabricated with Z26 as HTM, achieve a PCEs up to 20.1% under AM 1.5G (100 mW cm^{-2}) illumination. This approaches closely the PCE of 20.6 % obtained with spiro-OMeTAD. Moreover, the two HTMs based devices presented a better stability than that based on spiro-OMeTAD under ambient air condition of 30% or 85% relative humidity without encapsulation in the dark and under continuous full sun illumination at maximum power point tracking respectively.

The space helix structur of triphenylamine group as a terminal group can effectively prevent the π accumulation in the formation of accumulation , inhibiting the occurrence of crystallization. It can also reduce the direct contact between Au electrode and the light absorption layer, and thus effectively block the hole and electron recombination. The introduction of methoxy can improve the solubility of the material. When introducing the double bonds, the angles between the thiophene core ring and the attached benzene ring are 22.27 °and 12.09 ° for Z25 and Z26, respectively. Moreover, the angles between the benzene

groups of the terminal triphenylamine groups are 68.42 °and 68.62° for Z25 and Z26, respectively. It can be seen that the flatness of the Z26 molecule is better than that of Z25, thus, the conjugation effect is better which is more conducive to the transmission of holes.The Z25 was synthesized by Suzuki cross-coupling reaction and Z26 was synthesized by Horner-Wadsworth–Emmons reaction with cheap starting materials. The synthetic route for the HTMs is depicted in **Figure 1b** and experimental details are given in the supporting information. These two new thiophene derivatives were fully characterized by ^{1}H NMR spectroscopy, ^{13}C NMR spectroscopy and MALDI-TOF mass spectrum.All the analytical data are consistent with the proposed structures(**Figure S1−S6**). We also roughly estimated the synthesis cost of 1 gram Z25 and Z26 and the details are shown in the supporting information. The estimated synthesis cost of Z25 and Z26 is 31.91$/g and 31.70$/g, respectively which is much cheaper than that of spiro-OMeTAD (598 $/g). We have tested the UV-Vis absorption of the HTMs in CB solution with additives prepared freshly and after 8 days (**Figure S7**) and tested the ^{1}H NMR of HTMs with additives prepared freshly and after 8 days (**Figure S8**).There are no change in both UV-Vis absorption spectra and ^{1}H NMR specture after 8 days,indicating that precursor solution is stable under an ambient condition.

The normalized UV-Vis absorption and photoluminescence (PL) spectra of Z25 ,Z26 and spiro-OMeTAD in THF solution (1.0×10^{-5} mol L^{-1}) and spin-coated films are shown in **Figure 2**(a,b), and the corresponding data are summarized in **Table 1**. As shown in **Figure 2a**, Z25 and Z26 show the $\lambda_{abs}/_{max}$ around 390-460 nm,which is red-shifted compared to spiro-OMeTAD. The absorption bands in the 300-320 nm region can be assigned to the n-π* transition of the triphenylamine moieties.[43]The absorption at 396 nm of Z25 in solution is attributed to the π-π* transition of conjugated systerm of triphenylamine unit and thiophene ring,while the absorption in 456 nm of Z26 in solution is attributed to the π-π* transition of a

larger conjugated system formed by bridging the triphenylamine unit with the central dimethoxythiophene group via an ethylenic bond. [44] Due to the larger degree of conjugation produced by introducting two double bonds, [45] the $\lambda_{abs/max}$ of Z26 shows a red shift compared with regards to Z25. The spin-coating thin film absorption spectra are slightly broadened and red-shifted in comparison to that of solution state due to slightly strong intermolecular π-π stacking in the film. [46] The PL spectra of the thin films display a similar pattern as those of the solutions for the two HTMs, indicating absence of significant aggregation or crystallization in the solid films.[47]

Thermogravimetric analysis (TGA) and differential scanning calorimetry (DSC) measurements show that these two HTMs have high decomposition temperatures (T_d, 402 ºC and 377 ºC for Z25 and Z26, respectively) and glass transition temperatures (T_g, 77 ºC and 98 ºC for Z25 and Z26, respectively) (**Figure 2c**),which are comparable with that of spiro-OMeTAD[48]. The hole transporting properties of pristine HTMs were determined from hole-only devices using time-of-flight (TOF) measurements (**Figure S9a-c**). The obtained intrinsic hole mobility value of Z25, Z26 and spiro-OMeTAD are 7.66×10^{-5} cm^2 V^{-1} s^{-1},1.34×10^{-4} cm^2 V^{-1} s^{-1} and 4.32×10^{-4} cm^2 V^{-1} s^{-1} at an electric field of 1.5×10^5 V cm^{-1}, respectively. We also calculated the reorganization energies of Z25 and Z26. As indicated in **Table S2**, Z26 has the lower calculated reorganization energy than Z25, which agrees with the result of TOF test and indicates that the introduction of double bonds can enlarge the favor the transport [49]. The conductivity of these three doped HTMs were determined by a two-contact electrical conductivity set-up.[50] J–V curves and fitting results are shown in **Figure S9d**. The obtained doped conductivity value of Z25 and Z26 are 9.6×10^{-5} S cm^{-1} and 2.1×10^{-4} S cm^{-1}, respectively, which are comparable to that of spiro-OMeTAD (3.5×10^{-4} S cm^{-1}).

The optimized molecular geometries, the highest occupied molecular orbital (HOMO) levels and the lowest unoccupied molecular orbital (LUMO) energy levels were determined by density functional theory (DFT) calculations and shown in **Figure 2d**. The LUMO of these three HTMs distribute mainly on central core part while the HOMO energy levels distribute mainly on the entire molecular skeleton. The calculated HOMO levels of three HTMs are estimated to be -4.30 eV,-4.17 eV and -4.15 eV for Z25, Z26 and spiro-OMeTAD, while the LUMO levels are estimated to be -1.00 eV,-1.58 eV and -0.53 eV for Z25, Z26 and spiro-OMeTAD, respectively. We performed cyclic voltammetry (CV) measurement to determine their energy levels experimentally shown in **Figure 3a**. The data are summarized in **Table 1**. The HOMO energy levels of Z25 and Z26 are -5.18 eV and -5.16 eV , respectively, which are slightly lower than that of spiro-OMeTAD (-5.11 eV). The LUMO levels of HTMs are calculated to be -2.44 eV,-2.77 eV and -2.12 eV, which are more positive than that of mix-perovskite (-3.9 eV).[24] These results agreed well with the trend derived from DFT calculations.

The steady-state PL spectra are shown in **Figure 3c**. Strong PL quenching was observed when the HTM materials were coated on perovskite films. For the three HTMs coated perovskite films, the PL intensity was reduced to roughly 10%, 3% and 13% of that from pristine films for Z25, Z26 and spiro-OMeTAD respectively, suggesting that Z26 can extract charge carrier more efficiently than the other two HTMs. The hole extraction capacities at Glass/perovskite/HTMs interfaces have been investigated by time-resolved photoluminescence (TRPL) measurement. **Figure 3d** presents the measured PL decay spectra and the corresponding decay time are obtained by fitting the data with biexponential decay function.[51] In biexponential decay process, PL decay is related to recombination kinetics, where the short-lived life time (τ_1) in fast component correlates with surface property and/or non-radiative recombination whereas the long-lived life time (τ_2) in slow

component is related to bulk property.[52] The Z25/perovskite, Z26/perovskite and spiro-OMeTAD/perovskite film respectively show short-lived and long-lived lifetimes of (τ_1 = 0.5 ns , τ_2 = 2.2 ns) ,(τ_1 = 0.2 ns , τ_2 = 0.9 ns) and(τ_1 = 0.3 ns , τ_2 =1.2 ns) . By contrast, the pristine perovskite film gave τ_1 = 13.01 ns and τ_2 = 185.80 ns for these lifetimes. The PL decay lifetimes for the devices with Z25, Z26 or spiro-OMeTAD are significantly shorter than the device without HTM layer. It means that the Z25 and Z26 can extract the holes from the perovskite as efficient as spiro-OMeTAD.

To demonstrate the ability of Z25 and Z26 act as HTM, we prepared PSCs with configuration of FTO/TiO_2(compact)/TiO_2(mesoporous)/perovskite/HTM/Au, using a similar method as reported in our recent paper.[1] **Figure 4a** displays the cross-section images of the PSCs analyzed by field-emission scanning electron microscopy. The device is made of ~400 nm perovskite atop a ~200 nm thick mesoporous TiO_2 layer, which was deposited on FTO glass coated with ~60 nm compact TiO_2. The device is completed by an ~180 nm thick HTM and 80 nm gold film as a back contact. **Figure 4b** illustrates the current–voltage (J–V) traces collected under simulated solar illumination (AM 1.5, 100 mW cm^{-2}) for the best PSC among 20 devices and the photovoltaic parameters are summarized in **Table 2**.The best device based on Z25 affords an open-circuit voltage (V_{oc}) of 1.145 V, a short-circuit current density (J_{sc}) of 23.12 mA cm^{-2} and a fill factor (FF) of 0.64, leading to a PCE of 16.9 % ,while the Z26-based perovskite solar cells present the best performance with PCE of 20.1 %, J_{sc} of 23.59 mA cm^{-2}, V_{oc} of 1.132 V, and FF of 0.75 under AM 1.5G (100 mW cm^{-2}) illumination. This result is comparable to that of spiro-OMeTAD (20.6 %, J_{sc} of 23.87 mA cm^{-2}, V_{oc} of 1.130 V, and FF of 0.76). The stabilized power outputs from devices based on spiro-OMeTAD ,Z25 and Z26 are 20.4%, 16.7% and 19.8% respectively (**Figure 4d**), consistent with the obtained PCE. We also fabricated batches of 20 cells each using these two HTMs and spiro-OMeTAD and

demonstrate in **Figure 5** excellent reproducibility by the narrow statistical distribution of the photovoltaic metrics. The incident photon-to-electron conversion efficiency (IPCE) spectrum of the cell with the three HTMs is presented in **Figure 4c.** The integrated current densities estimated from the IPCE spectra (22.14 mA cm^{-2}, 22.76 mA cm^{-2} and 22.99 mA cm^{-2} for Z25, Z26 and spiro-OMeTAD, respectively) are in good agreement with the J_{sc} values obtained from the J-V curves.

The stability of PSCs is a key factor that plays a major role in their commercialization potential. **Figure 6** shows the stability tests of corresponding perovskite solar cells in ambient environment of 30% relatively humidity without encapsulation and under continuous full sun illumination at maximum power point tracking in a nitrogen atmosphere at room temperature without encapsulation, respectively. **Figure S10** shows the stability tests of corresponding perovskite solar cells in ambient environment of 85% relatively humidity without encapsulation, in ambient environment of 40% relatively humidity under dark without encapsulation at 65℃ and under continuous full sun illumination at maximum power point tracking in ambient environment of 40% relatively humidity with encapsulation at room temperature, respectively. Obviously, the devices based on Z26/25 present a better stability than that of spiro-OMeTAD based perovskite solar cell. As shown in **Figure 6a**, the PCE maintained 85.5% of the initial value in the Z26-based perovskite solar cell, whereas it decreased to 46.5% and 66.8% of the initial value in the spiro-OMeTAD based perovskite solar cell and Z25-based perovskite based solar cells after 800 h. **Figure 6b** indicates that there is 14% , 42% and 87% efficiency drop after 300 h under continuous full sun illumination and maximum power point tracking for Z26,Z25 and spiro-OMeTAD-based perovskite solar cell, respectively. Moreover, preliminary tests in **Figure S10** shows that Z26-based device is more resistant to higher humidity and heat stress than the device based on Z25

and spiro-OMeTAD. We ascribed the improvement of stability based on Z26 mainly to the presence of less pinholes in the HTM layer (**Figure S11-S12**), more hydrophobic nature (**Figure S13**) and enhanced interfacial coupling between Z26 and perovskite through the thiophene–iodine enhancing hole collection by the HTM.[25,46,50] As a result, the Z26-based perovskite based device showed a much stronger resistance to degradation over longer time periods than the other two corresponding HTM –based devices.

In summary, we synthesized two novel thiophene-cored HTMs (Z25 and Z26) with simple low cost process. Z26 presents a more homogeneous surface, higher hole mobility and higher conductivity than Z25 by introduction of double bonds. The perovskite solar cell based on Z26 as HTM affords an impressive PCE of 20.1 %, which is comparable to that obtained employing the well-known spiro-OMeTAD. The devices based on Z26 also obtained a higher stability than that of Z25 and spiro-OMeTAD at room temperature aged under ambient air of 30% or 85% relative humidity without encapsulation in the dark and under continuous full sun illumination at maximum power point tracking, respectively. Moreover, the cost of these HTMs is around 1/20 of that of spiro-OMeTAD. The introduction of double bonds into HTMs with easier synthesis, low cost and excellent performance highlight this simple strategy to design potential HTMs in the future deployment of highly efficient and stable perovskite solar cells.

Supporting Information

Supporting Information is available from the Wiley Online Library or from the author.

Acknowledgements

This work was supported by the the National Natural Science Foundation of China (21676188) and Key Projects in Natural Science Foundation of Tianjin (16JCZDJC37100).FZ thanks the China Scholarship Council and the Collaborative Innovation Center of Chemical Science and Engineering (Tianjin) for funding. MG. and SMZ thank the King Abdulaziz City for Science and Technology (KACST) for financial support. Financial support from the Swiss National Science Foundation (SNSF), the NRP 70 "Energy Turnaround", CCEM-CH in the 9th call proposal 906: CONNECT PV, the European Union's Horizon 2020 research and innovation programme under the grant agreement No 687008 (GOTSolar) as well as from SNF-NanoTera and Swiss Federal Office of Energy (SYNERGY) are also gratefully acknowledged.

F.Z. and D.Q.B designed the experiment. F.Z carried out the experimental study on device fabrication and performed basic characterization. Z.Q.W and Y.X designed and synthesized the two hole-transporting material, also performed all the physical property tests and quantum chemical calculation. X.C.L tested the mobility. H.W.Z calculated the cost of HTMs and performed AFM test. F.Z. performed the PL test. N.P, D.Q.B and Y.C.Y performed the stability test. J.S.L. performed SEM measurements. Z.F wrote the first draft of the paper. All the authors contributed to the discussion and the writing of the paper, and approved. S.M.Z. and X.G.L coordinated the research, whereas S.R.W. and M.G. supervised the project.

Received: ((will be filled in by the editorial staff))
Revised: ((will be filled in by the editorial staff))
Published online: ((will be filled in by the editorial staff))

[1]D. Q.Bi, W.Tress, M.I.Dar, P.Gao, J.S.Luo, C.Renevier, K.Schenk,A.Abate, F.Giordano, J.C.Baena, J.Decoppet, S.M.Zakeeruddin, M.K.Nazeeruddin, M.Grätzel, A.Hagfeldt, *Sci. Adv.* **2016**, 2, e1501170.

[2]F. Zhang, S.R.Wang, X.G.Li, Y.Xiao, *Curr. Nanosci.* **2016**, 12, 137.

[3]F.Zhang, S.R.Wang, X.G.Li, Y.Xiao, *Synthetic Metals*.**2016**, 220, 187.

[4]P.Qi, F. Zhang, Y.Xiao,X. Li, J.J.Guo, S. Wang, *Synthetic Metals,***2017**,226,1.

[5]D.Q.Bi, C.Y.Yi, J.S.Luo, J.D. Décoppet, F.Zhang, S.M. Zakeeruddin, X. Li, A.Hagfeldt , M.Grätzel, *Nature Energy* ,**2016**, 1, 16142.

[6]Z.Yu,L.C.Sun, *Adv.EnergyMater*.**2015**, 5, 1500213.

[7]K. Rakstys, M. Saliba, P. Gao, P. Gratia, E. Kamarauskas, S.Paek, V. Jankauskas, M. K. Nazeeruddin, *Angew. Chem.Int. Ed.* **2016**, 55, 7464.

[8]P. Gratia, A. Magomedov, T. Malinauskas, M. Daskeviciene,A. Abate, S. Ahmad, M. Grätzel, V. Getautis, M. K.Nazeeruddin, *Angew. Chem. Int. Ed.* **2015**, 54, 11409.

[9]M. H. Li, C. W. Hsu, P. S. Shen, H. M. Cheng, Y. Chi, P. Chen, T.F. Guo, *Chem. Commun.* **2015**, 51, 15518.

[10]S. Park, J. H. Heo, J. H. Yun, T. S. Jung, K. Kwak, M. J. Ko, C. H.Cheon, J. Y. Kim, S. H. Im, H. J. Son, *Chem. Sci.* **2016**, 7, 5517.

[11]H. Nishimura, N. Ishida, A. Shimazaki, A. Wakamiya, A. Saeki,L. T. Scott, Y. Murata, *J. Am. Chem. Soc.* **2015**, 137, 15656.

[12]K. Rakstys, A. Abate, M. I. Dar, P. Gao, V. Jankauskas, G.Jacopin, E. Kamarauskas, S. Kazim, S. Ahmad, M. Grätzel, M.K. Nazeeruddin, *J. Am. Chem. Soc.* **2015**, 137, 16172.

[13]D. Bi, A. Mishra, P. Gao, M. Franckevičius, C. Steck, S. M.Zakeeruddin, M. K. Nazeeruddin, P. Bäuerle, M. Grätzel, A. Hagfeldt, *ChemSusChem*. **2016**, 9, 433.

[14]Y.K. Wang, Z.C. Yuan, G.Z. Shi, Y.X. Li, Q. Li, F. Hui, B.Q.Sun, Z.Q. Jiang, L.S. Liao, *Adv. Funct. Mat.* **2016**, 26,1375.

[15]C. Huang, W. Fu, C.-Z. Li, Z. Zhang, W. Qiu, M. Shi, P.Heremans, A. K.-Y. Jen, H. Chen, *J. Am. Chem.Soc.* **2016**, 138 (8), 2528.

[16]Z. Hu, W. Fu, L. Yan, J. Miao, H. Yu, Y. He, O. Goto, H. Meng,H. Chen, W. Huang, *Chem. Sci.*, **2016**, 7, 5007.

[17]A. Molina-Ontoria, I. Zimmermann, I. Garcia-Benito, P.Gratia, C. Roldán-Carmona, S. Aghazada, M. Graetzel, M. K.Nazeeruddin, N. Martín, *Angew. Chem. Int. Ed.* **2016**, 55,6270.

[18]J. Zhang, B. Xu, M. B. Johansson, M. Hadadian, J. P. CorreaBaena, P. Liu, Y. Hua, N. Vlachopoulos, E. M. J. Johansson, G.Boschloo, L. Sun, A. Hagfeldt, *Adv. Energy. Mat.* **2016**, 6,1502536.

[19]Y. Hua, J. Zhang, B Xu, P. Liu, M. Cheng, L. Kloo, E. M.J.Johansson, K. Sveinbjörnsson, K. Aitola, G. Boschloo, L.Sun, *Nano Energy*. **2016**, 26, 108.

[20]F. Zhang, C. Yi, P. Wei, X. Bi, J. Luo, G. Jacopin, S. Wang, X. Li,Y. Xiao, S. M. Zakeeruddin, M.Grätzel, *Adv. Energy. Mat.* **2016**, 6, 1600401.

[21]J. Zhang, B. Xu, M. B. Johansson, N. Vlachopoulos, G.Boschloo, L. Sun, E. M. J. Johansson, A. Hagfeldt, *ACS Nano*. **2016**, 10 , 6816.

[22]S. Paek, I. Zimmermann, P. Gao, P. Gratia, K. Rakstys, G.Grancini, M. K. Nazeeruddin, M. A. Rub, S. A. Kosa, K. A.Alamry, A. M. Asiri, *Chem. Sci.* **2016**, 7, 6068.

[23]F. Zhang, X. Liu, C. Yi, D. Bi, J.Luo, S. Wang, X. Li, Y.Xiao, S. Zakeeruddin, M. Grätzel, *ChemSusChem*. **2016**,9, 2578.

[24]I.Zimmermann, J.Urieta-Mora, P.Gratia, J.Aragó, G.Grancini,A.Molina-Ontoria,E.Ortí, N.Martín, M.K.Nazeeruddin, *Adv. Energy Mater.* **2016**, 1601674.

[25] M. Saliba, S. Orlandi, T. Matsui, S. Aghazada, M. Cavazzini, J.P. Correa-Baena, P. Gao, R. Scopelliti, E. Mosconi, K. H.Dahmen, F. De Angelis, A. Abate, A. Hagfeldt, G. Pozzi, M.Graetzel, M. K. Nazeeruddin, *Nature Energy*. **2016**,15017.

[26]B. Xu, D. Bi, Y. Hua, P. Liu, M. Cheng, M. Grätzel, L. Kloo, A.Hagfeldt, L. Sun, *Energy Environ. Sci.* **2016**, 9, 873.

[27]D. Bi, B. Xu, P. Gao, L. Sun, M. Grätzel, and A. Hagfeldt, *Nano Energy*. **2016**, 23, 138.

[28]T. Malinauskas, M. Saliba, T. Matsui, M. Daskeviciene, S.Urnikaite, P. Gratia, R. Send, H. Wonneberger, I. Bruder, M.Graetzel, V. Getautis, M. K. Nazeeruddin, *Energy Environ.Sci.* **2016**, 9, 1681.

[29]K.Rakstys, S.Paek, M.Sohail, P.Gao, K.T.Cho, P.Gratia, Y.Lee, K.H.Dahmen, M.K.Nazeeruddin, *J. Mater. Chem. A*. **2016**, 4, 18259.

[30]H.S. Kim, I. Mora-Sero, V. Gonzalez-Pedro, F. Fabregat-Santiago, E.J. JuarezPerez, N.G. Park, J. Bisquert, *Nat. Commun.***2013**, 4, 2242.

[31]J.M. Frost, K.T. Butler, F. Brivio, C.H. Hendon, M. Schilfgaarde, A. Walsh,*Nano. Lett.* **2014**,14,2584.

[32]S. Park, J.H. Heo, C.H. Cheon, H. Kim, S.H. Im, H.J. Son, *J. Mater. Chem. A*. **2015**, 3, 24215.

[33] B. Xu, H. Tian, D. Bi, E. Gabrielsson, E.M.J. Johansson, G. Boschloo, A. Hagfeldt,L. Sun, *J. Mater. Chem. A*. **2013**,1, 14467.

[34]L.Calio, S.Kazim, M.Gratzel, S.Ahmad, *Angew. Chem. Int. Ed.* **2016**, 55, 14522.

[35]M. L. Petrus, T. Bein, T. J. Dingemans, P. Docampo, *J. Mater.Chem. A*. **2015**, 3, 12159.

[36]H. Li, K. Fu, A. Hagfeldt, M. Gratzel, S. G. Mhaisalkar, A. C.Grimsdale, *Angew. Chem. Int. Ed.* **2014**, 53, 4085;*Angew. Chem.* **2014**, 126, 4169.

[37]T. Krishnamoorthy, F. Kunwu, P. P. Boix, H. Li, T. M. Koh,W. L. Leong, S. Powar, A. Grimsdale, M. Gratzel, N. Mathews S.G. Mhaisalkar, *J. Mater. Chem. A*. *2014*, 2, 6305.

[38]H. Li, K. Fu, P. P. Boix, L. H. Wong, A. Hagfeldt, M. Gratzel,S. G. Mhaisalkar, A. C. Grimsdale, *ChemSusChem*. **2014**, 7,3420.

[39]H. Wang, A. D. Sheikh, Q. Feng, F. Li, Y. Chen, W. Yu, E.Alarousu, C. Ma, M. A. Haque, D. Shi, Z.S.Wang, O.F. Mohammed, O.M. Bakr, T.Wu, *ACS Photonics*. **2015**, 2, 849.

[40]P. Ganesan, K. Fu, P. Gao, I. Raabe, K. Schenk, R. Scopelliti, J.Luo, L. H. Wong, M. Gratzel, M. K. Nazeeruddin, *Energy Environ. Sci.* **2015**, 8, 1986.

[41]M. Franckevicius, A. Mishra, F. Kreuzer, J. Luo, S. M.Zakeeruddin, M. Gratzel, *Mater. Horiz.* **2015**, 2, 613.

[42]A. Abate, S. Paek, F. Giordano, J. P. C. Baena, M. Saliba, P.Gao, T. Matsui, J. Ko, S. M. Zakeeruddin, K. H. Dahmen ,A. Hagfeldt, M.Grätzela ,M.K. Nazeeruddin ,*Energy Environ. Sci.* **2015**, 8, 2946.

[43] P.Qi,F. Zhang, X. Zhao, X. Bi, P. Wei,Y.Xiao,X. Li, S. Wang ,*Energy Technol*. **2017**, DOI:10.1002/ente.201600517.

[44]S. Karthikeyan, M. Thelakkat, *Inorg. Chim. Acta.* **2008**, 36, 635

[45]I. Neogi, S. Jhulki, M. Rawat, R.S. Anand, T. J. Chow, J. N. Moorthy, *RSC Adv.* **2015**, 5, 26806.

[46] X.M. Zhao,F.Zhang, C.Y. Yi, D.Q. Bi, X.D. Bi, P. Wei,J.S.Luo, X.C.Liu, S.R.Wang, X.G.Li, S.M.Zakeeruddin, M. Grätzel,*J. Mater. Chem. A*. **2016**, 4, 16330.

[47]Y. Kim, C.W. Joo, J. Lee, J.C. Woo, J.Y. Oh, N. S. Baek, H. Y. Chu ,J.I. Lee, *RSC Adv.* **2015**, 5, 8415-8421.

[48]S. Park, J. H. Heo, C. H. Cheon, H. Kim, S. H. ImH. J. Son, *J. Mater. Chem. A*, **2015**, 3, 24215.

[49] F.Zhang, X.M. Zhao, C.Y. Yi, D.Q. Bi, X.D. Bi, P. Wei, X.C.Liu, S.R.Wang, X.G.Li, S.M.Zakeeruddin, M. Grätzel, *Dyes and Pigments.* **2017**, 136, 273.

[50]H. J. Snaith, M. Gratzel, *Appl. Phys. Lett.* **2006**, 89,262114.

[51]X.C.Liu, L.F.Zhu, F.Zhang, J.You, Y.Xiao, D.M.Li, S.R.Wang, Q.B.Meng, X.G.Li. *Energy Technol.* **2017**,5, 312–320.

[52] D. Shi, V. Adinolfi, R. Comin, M.Yuan, E.Alarousu, A.Buin, Y.Chen, S.Hoogland, A.Rothenberger, K.Katsiev, Y.Losovyj, X.Zhang, P. A.Dowben,O. F.Mohammed, E. H. Sargent, O. M.Bakr, *Science*, **2015**, 347, 519.

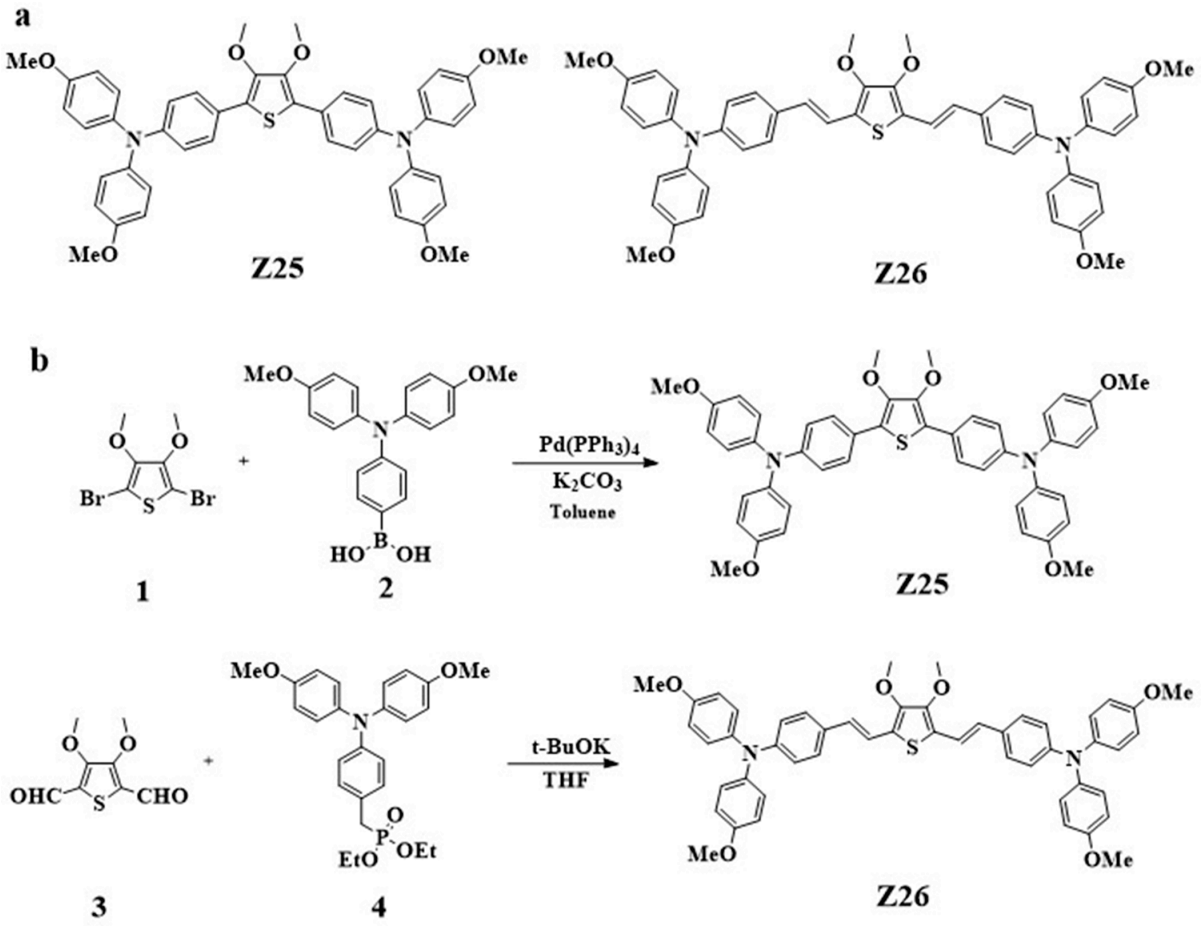

Figure 1 (a) Molecular structures of two HTMs; (b) Synthetic route for two HTMs.

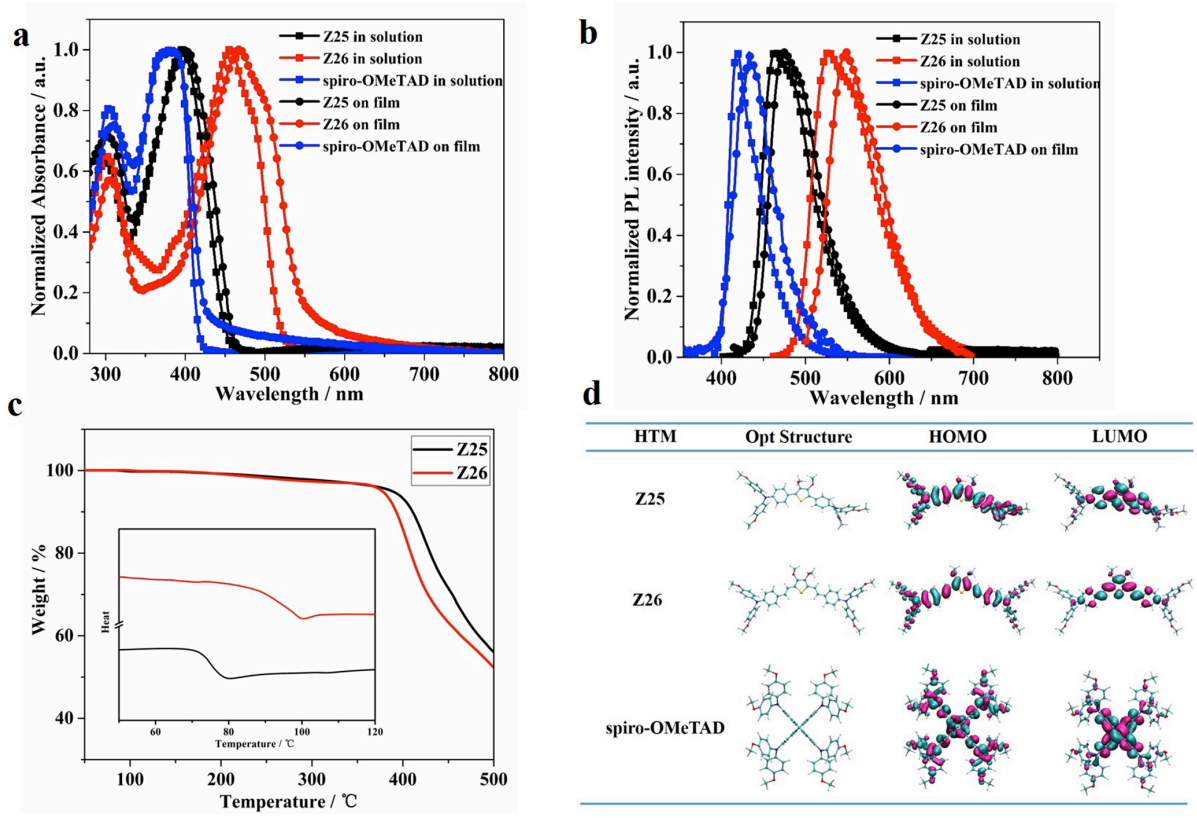

Figure 2 (a) Normalized UV-Vis absorption spectra of the HTMs in THF solution(c = 1.0×10^{-5} mol L^{-1}) and on film ; (b) Normalized photoluminescence spectra of HTM films in THF solution(c = 1.0×10^{-5} mol L^{-1}) and on film ; (c) DSC and TGA curves of the two HTMs; (d) The calculated frontier molecular orbitals of HTMs.

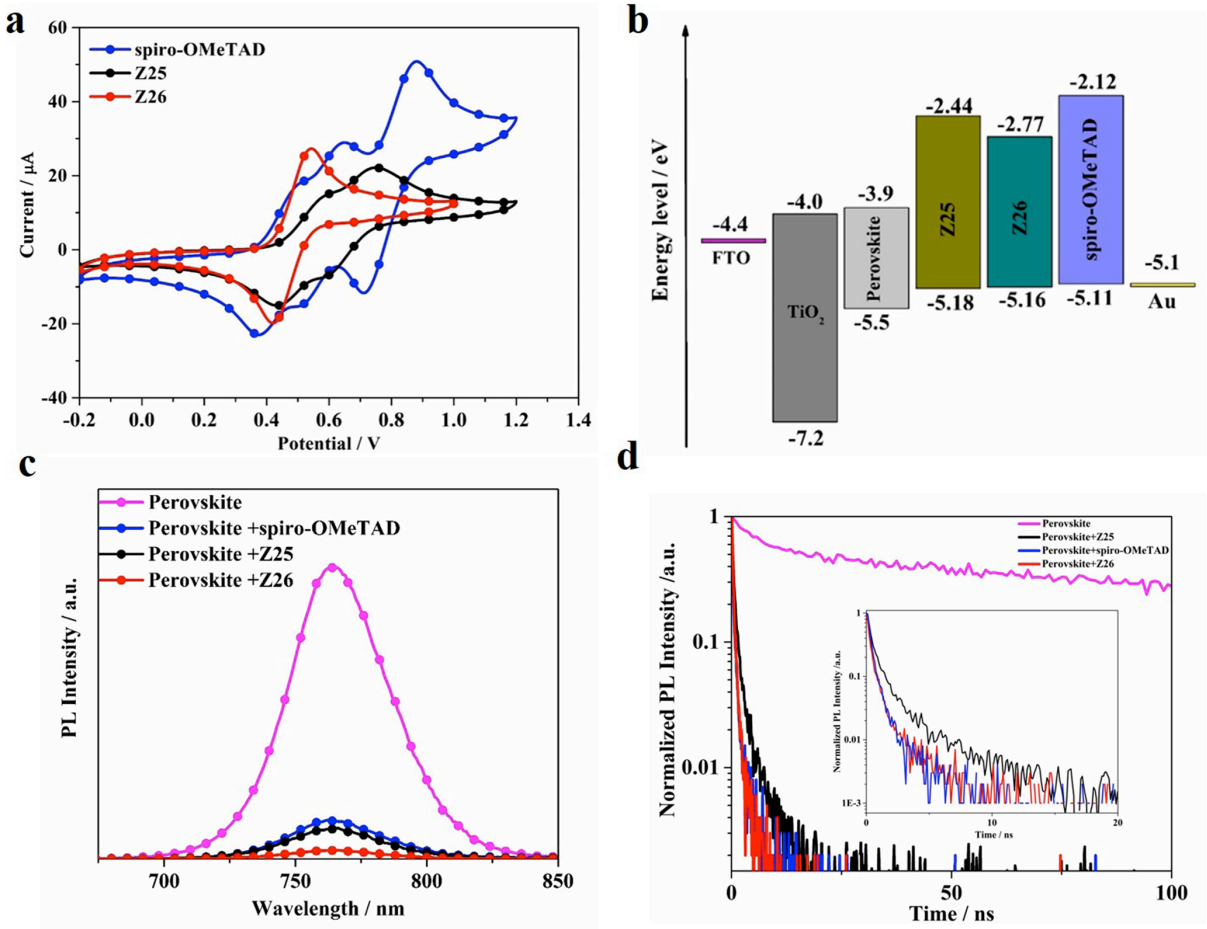

Figure 3 (a) CV curves of HTMs in dichloromethane solution ; (b) Energy level diagram of the corresponding materials used in perovskite solar cells;(c) PL spectra, (d) TRPL spectra of corresponding films on glass substrate.The inset is enlarged TRPLspectra of different HTMs on perovskite film.

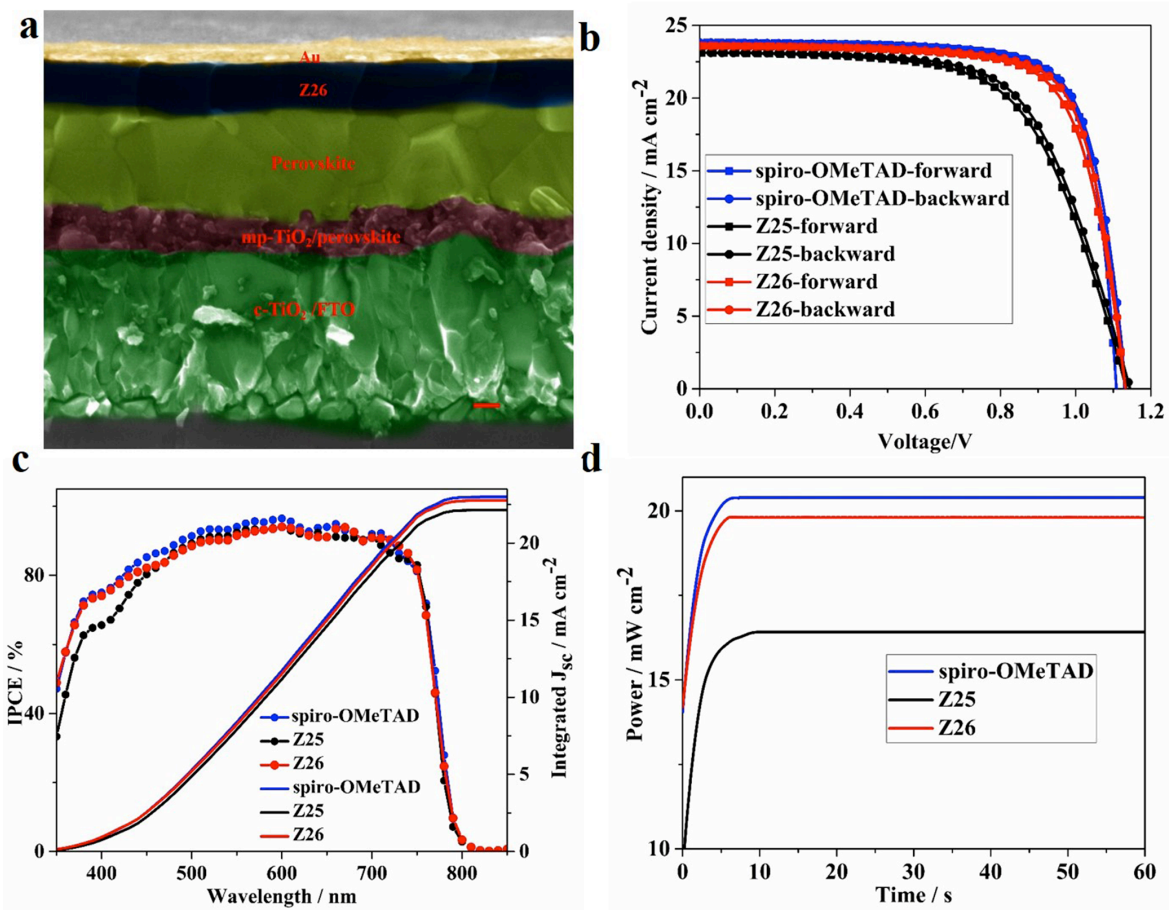

Figure 4 (a) Cross-sectional SEM image of the device based on Z26.The scale bar is 200 nm ; (b) Current-voltage hysteresis curves of perovskite solar cells comprising champion devices measured starting with backward scan and continuing with forward scan ; (c) IPCE spectra and integrated current curves of the corresponding devices ; (d) The stabilized power output of the corresponding devices.

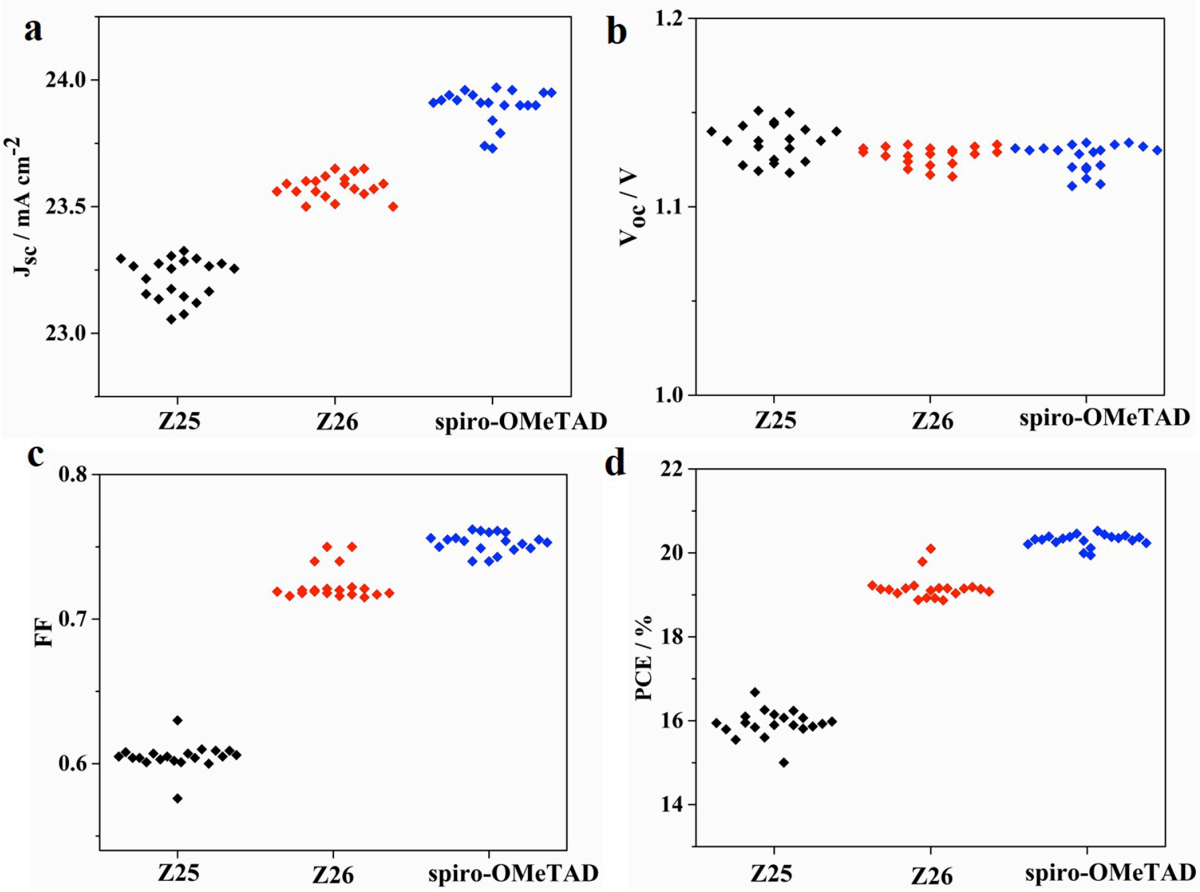

Figure 5 Photovoltaic metrics of devices based on corresponding HTM-based perovskite solar cells

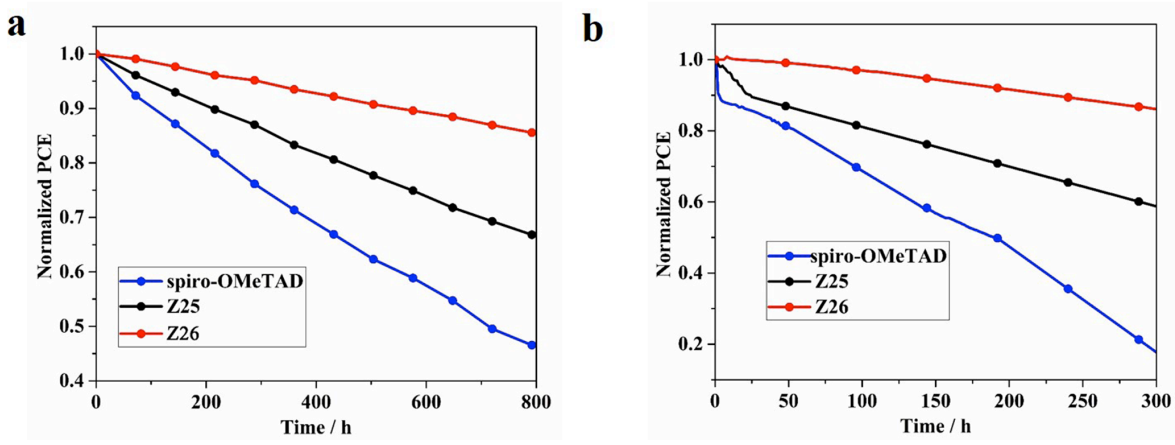

Figure 6 The stability of corresponding perovskite solar cells (a) in ambient environment of 30% relatively humidity under dark without any encapsulation at room temperature. (b) under

continuous full sun illumination and maximum power point tracking in a nitrogen atmosphere at room temperature .

Table 1 Photophysical, electrochemical data and thermal characteristics of two HTMs

HTM	$\lambda_{abs/max}$ (nm)	E_g(eV)	HOMO(eV)	LUMO(eV)	T_d(ºC)	T_g(ºC)
Z25	396[a] /397[b]	2.74[c] 3.30[d]	-5.18[c] -4.30[d]	-2.44[c] -1.00[d]	402	77
Z26	456[a] /469[b]	2.39[c] 2.59[d]	-5.16[c] -4.17[d]	-2.77[c] -1.58[d]	377	98
spiro-OMeTAD	378[a] /380[b]	2.99[c] 3.62[d]	-5.11[c] -4.15[d]	-2.12[c] -0.53[d]	452[48]	124[48]

[a)]: UV-Vis absorption of THF solution(c = 1.0×10^{-5} mol L^{-1}) ;[b)]: UV-Vis absorption of the films; [c)]: experiment calculation values (HOMO levels is measured by CV); [d)]:theoretical calculation values.

Table 2 *J-V* curves of HTMs based champion devices under different scan directions with bias step of 5 mV

HTM		J_{sc}(mA cm^{-2})	V_{oc}(V)	*FF*	PCE(%)
spiro-OMeTAD	backward	23.87	1.130	0.76	20.6
	forward	23.87	1.109	0.77	20.4
Z25	backward	23.12	1.145	0.64	16.9
	forward	23.12	1.135	0.63	16.4
Z26	backward	23.59	1.132	0.75	20.1
	forward	23.59	1.133	0.73	19.7

Two novel and low-cost thiophene-based hole transporting materials were designed and synthesized. The newly developed Z26 based perovskite solar cell exhibited a remarkable PCE of 20.1 % along with enhanced stability under ambient air and illumination.

Keyword: stability; thiophene; hole transporting materials; perovskite solar cell

Fei Zhang ,Zhiqiang Wang, Hongwei Zhu, Norman Pellet,Jingshan Luo, Chenyi Yi, Xicheng Liu,Shirong Wang, Xianggao Li , Yin Xiao, Shaik Mohammed Zakeeruddin* , Dongqin Bi*, Michael Grätzel**

Over 20% PCE perovskite solar cells with superior stability achieved by novel and low-cost hole-transporting materials

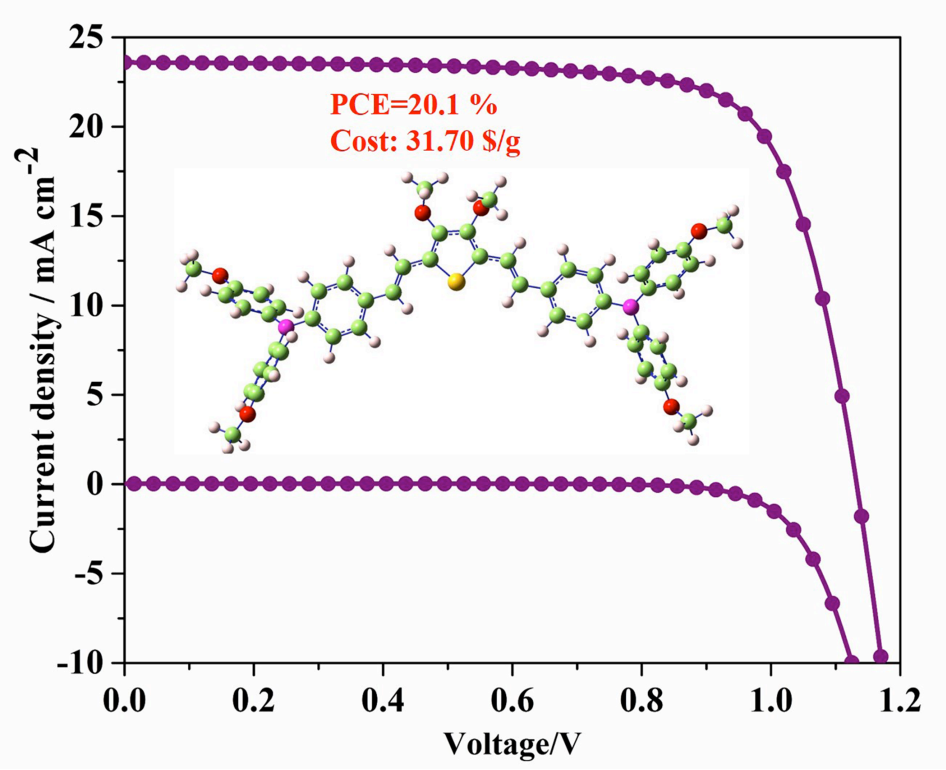

Supporting Information

Over 20% PCE perovskite solar cells with superior stability achieved by novel and low-cost hole-transporting materials

Fei Zhang ,Zhiqiang Wang, Hongwei Zhu, Norman Pellet,Jingshan Luo, Chenyi Yi, Xicheng Liu,Shirong Wang, Xianggao Li , Yin Xiao, Shaik Mohammed Zakeeruddin* , Dongqin Bi*, Michael Grätzel**

F. Zhang, Z.Wang,H.Zhu,Dr.Y.Xiao, Prof. S. Wang ,Prof. X. Li, *
School of Chemical Engineering and Technology, Tianjin University
300072 Tianjin, China
Email: lixianggao@tju.edu.cn

F. Zhang, N.Pellet, Dr. J. Luo, Dr. C. Yi, Dr. S. M. Zakeeruddin, Dr. D. Bi , Prof. M. Grätzel*
Laboratory of Photonics and Interfaces, Institute of Chemical Sciences and Engineering,
École Polytechnique Fédérale de Lausanne (EPFL)
Station 6 CH-1015, Lausanne, Switzerland
Email: shaik.zakeer@epfl.ch ; dongqin.bi@epfl.ch ; michael.graetzel@epfl.ch

F. Zhang, Z.Wang,H.Zhu,Dr.Y.Xiao, Prof. S. Wang ,Prof. X. Li, *
Collaborative Innovation Center of Chemical Science and Engineering(Tianjin)
300072 Tianjin, China

Dr.X.Liu
Qufu Normal University, School of Chemistry and Chemical Engineering,
273165 Qufu, China

N.Pellet
Max Planck Institute for Solid State Research
Heisenbergstrasse 1, Stuttgart 70569, Germany

*Materials:*Materials were all available commercially and used without further purification if not mentioned specially.

Materials measurements:^{1}H NMR spectras was recorded with an INOVA 400MHz spectrometer (Varian, USA). Mass spectra (MS) was performed on an Autoflex tof/tofIII mass spectrometer (Bruker, Germany). UV spectra of the HTMs in tetrahydrofuran (THF) solutions (1×10^{-5} mol L^{-1}) was recorded with Thermo Evolution 300 UV-Vis spectrometer (Thermo Electron, USA) in the 200-800 nm wavelength range at room temperature. Thermo gravimetrical analyses (TGA) were recorded with TA Q500 thermo gravimetric apparatus (TA Instruments, USA) at a heating rate of 10 °C min^{-1} under nitrogen atmosphere. Differential scanning calorimetry (DSC) was conducted on TA Q20 Instrument (TA Instruments, USA) at a heating rate of 10 °C min^{-1} under nitrogen atmosphere.

The cyclic voltammetry measurements were performed on a Zahner Elektrik IM6e electrochemistry workstation (Zahner, Germany) with a three-electrode system in dry dichloromethane in the presence of tetrabutylammonium hexafluorophosphate (n-Bu4NPF6, 0.1M) as supporting electrolyte with a scanning rate of 100mV/s at room temperature. The platinum electrode (Pt 213) was used as the working electrode and the auxiliary electrode, and the saturated calomel electrode was used as the reference electrode.The ferrocene/ferrocenium redox couple was applied as an external standard.

Time-of-flight measurement : The time-of-flight (TOF) measurement was recorded on a TOF401 instrument (Sumitomo Heavy Industries. Ltd., Japan). HTM layers with ~ 1 μm thickness were prepared through vacuum deposition onto ITO substrates and contacte witj a 100 nm aluminum layer with an active area of 3×10 mm^{2}. **Figure S7a-c** displays typical room-temperature TOF transients of holes for Z25,Z26 and spiro-OMeTAD under an applied

field of ~1.5×10^5 V cm^{-1}. The transit times (t_T) were obtained from the intersection point of two asymptotes in the double-logarithmic representations (insets of **Figure S7a-c**).

*The caculation of reorganization energy :*Reorganization energy(λ)=（E*）-E +（E+ *）-（E+）, where E+ and E are the optimized energies of the cationic and neutral forms of a single monomer, E+ * is the energy of the monomer cation at the neutral geometry, and E* is the energy of the neutral monomer at the cation geometry.λ1=（E+ *）-（E+）: Relaxation energy computed from the cation potential energy surface.λ2=（E*）-E: Relaxation energy computed from the neutral potential energy surface.

Synthesis of HTMs

4,4'-(3,4-dimethoxythiophene-2,5-diyl)bis(N,N-bis(4-methoxyphenyl)aniline) (Z25)

Compound **1** (0.577 g (1.9 mmol) ,**2** (1.4 g,4.0 mmol), anhydrous potassium carbonate(1.32 g ,9.6 mmol), 4-triphenylphosphine palladium(0.088 g ,0.08 mmol),50 mL of toluene and 5 mL of water were added into a 100mL round-bottom flask under N_2..The reaction solution was heated to reflux for 8 h and protected from light.After that, the product was purified by chromatographed on a silica gel column (petroleum ether: ethyl acetate =20:1 as eluent) to give yellow compound as a pure compound Z25 (0.77 g, 53.85%). M.p. = 90-93 °C. ^{1}H NMR (400 MHz, DMSO) δ 7.49 (d, J = 7.3 Hz, 4H), 7.07 (dd, J = 8.7, 2.8 Hz, 8H), 6.95 (dd, J = 4.9, 3.7 Hz, 8H), 6.81 (d, J = 8.6 Hz, 4H), 3.80 (d, J = 1.6 Hz, 6H), 3.77 (d, J = 1.8 Hz, 12H). ^{13}C NMR (101 MHz, DMSO) δ 156.40, 148.04, 146.37, 140.20, 127.37, 127.29, 124.25, 121.92, 119.45, 115.46, 60.47, 55.70. MS (MALDI-TOF): m/z calcd for $C_{46}H_{42}N_2O_6S$: 750.28 $[M]^+$; found: 750.55 $[M]^+$.

4,4'-((1E,1'E)-(3,4-dimethoxythiophene-2,5-diyl)bis(ethene-2,1-diyl))bis(N,N-bis(4-methoxyphenyl)aniline) (Z26)

Compound **3** (4.19 g ,9.2 mmol) and **4** (0.92 g ,4.6 mmol) were added into a 100mL round-bottom flask under N_2.Anhydrous THF (30 mL) was added to above flask, cooled down to 0 °C. The 10 mL THF solution of t-BuOK (1.29 g ,0.011 mol)) was added dropwise to above flask, stirred for 30 min at 0 °C, followed by stirring at room temperature for 12 h.After removing the solvent by evaporation,the residue was dissolved in 30 mL of methylene chloride. The mixture was extracted with 20 mL of deionized water and a small amount of dilute hydrochloric acid. The organic layer was extracted three times with dichloromethane, dried by anhydrous magnesium sulfate and the solvent was removed by evaporation After that, the product was purified by chromatographed on a silica gel column (petroleum ether: ethyl acetate =40:1,20:1 as eluent) to give orange compound as a pure compound Z26 (1.96g, 53.12%). ^{1}H NMR (400 MHz, $CDCl_3$) δ 7.27 (d, J = 8.6 Hz, 4H), 7.06 (dd, J = 12.7, 7.2 Hz, 10H), 6.88 (d, J = 8.6 Hz, 4H), 6.82 (d, J = 8.9 Hz, 8H), 6.73 (d, J = 16.0 Hz, 2H), 3.89 (s, 6H), 3.79 (s, 12H). ^{13}C NMR (101 MHz, $CDCl_3$) δ 155.99, 148.22, 147.39, 140.69, 129.44, 127.05, 126.66, 126.34, 123.43, 120.46, 115.60, 114.73, 61.31, 55.51. MS (MALDI-TOF): m/z calcd for $C_{50}H_{46}N_2O_6S$: 802.31 $[M]^+$; found: 802.45 $[M]^+$.

*Solar cell fabrication:*Devices were prepared on conductive fluorine-doped tin oxide (FTO) coated glass substrates. The substrates were cleaned extensively by deionized water, acetone and isopropanol. A compact titanium dioxide (TiO_2) layer was deposited by spray pyrolysis of 7 ml 2-propanol solution containing 0.6 mL titanium diisopropoxide bis(acetylacetonate) solution and 0.4 mL acetylacetone at 450 ℃ in air. On top of this layer, a 200-300 nm-thick mesoporous titanium dioxide was formed by spin-coating nanoparticles (30NRT, Dyesol) diluted in ethanol (1:5.5 *w*/*w*) at 4500 r.p.m. for 15 s. The formed layer was heated to 500 degrees and sintered for 0.5 h in oxygen atmosphere. The $[(FAI)_{0.81}(PbI_2)_{0.85}(MABr)_{0.15}(PbBr_2)_{0.15}]$ precursor solution was prepared in a glovebox from

a 1.35M Pb^{2+}(PbI_2 and $PbBr_2$) in the mixed solvent of DMF and DMSO, the volume ratio of DMF/DMSO is 4:1. The spin-coating procedure was performed by 2000 rpm for 10 s followed with 6000 rpm for 30 s. At 15 s before the last spin-coating step, 100 ml of chlorobenzene was pipetted onto the substrate. Thereafter, the substrate was put onto a hotplate for 1 hour at 100°C. Subsequently, the HTM were deposited on the top of perovskite by spin coating at 4000 r.p.m. for 15 s. The HTM solutions were prepared dissolving the HTM in 1 mL chlorobenzene at concentration of dissolving the spiro-OMeTAD or Z25 or Z26 in chlorobenzene at a concentration of 60 mM, with the addition of 30 mM lithium bis(trifluoromethanesulfonyl)imide from a stock solution in acetonitrile) containing 200 mM of tert-butylpyridine. FK209 (Dyenamo AB) was added to the HTM solution, from a stock solution in acetonitrile, the molar ratio of FK209 and HTM was 0.03.The HTM layer was deposited on the top of perovskite by spin coating at 4000 r.p.m. for 15 s. Devices were finalized by thermal evaporation of 80 nm thick gold layer.

J-V Characterization: The J-V characteristics of the devices were measured under 100mW/cm^2 conditions using a 450 W Xenon lamp (Oriel), as a light source, equipped with a Schott K113 Tempax sunlight filter (Praezisions Glas & Optik GmbH) to match the emission spectra to the AM1.5G standard in the region of 350-750 nm. The current–voltage characteristics of the devices were obtained by applying external potential bias to the cell while recording the generated photocurrent 3 using a Keithley (Model 2400) digital source meter. The J–V curves of all devices were measured by masking the active area with a metal mask of area 0.16 cm^2.

Long term light soaking test: Stability measurements were performed with a Biologic MPG2 potentiostat under a full AM 1.5 Sun-equivalent white LED lamp. The devices were measured with a maximum power point (MPP) tracking routine under continuous illumination (and

nitrogen). The MPP was updated every 10 s by a standard perturb and observe method. Every 1 minutes a JV curve was recorded in order to track the evolution of individual JV parameters.

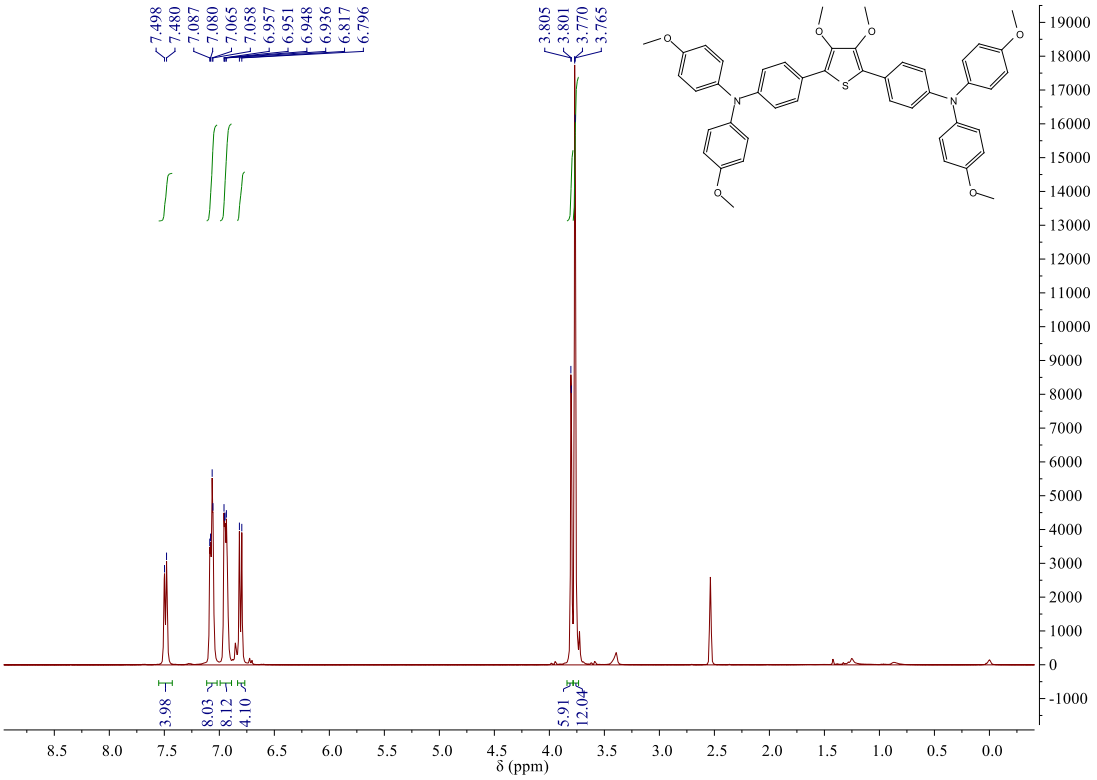

Figure S1. ^{1}H NMR spectrum of Z25

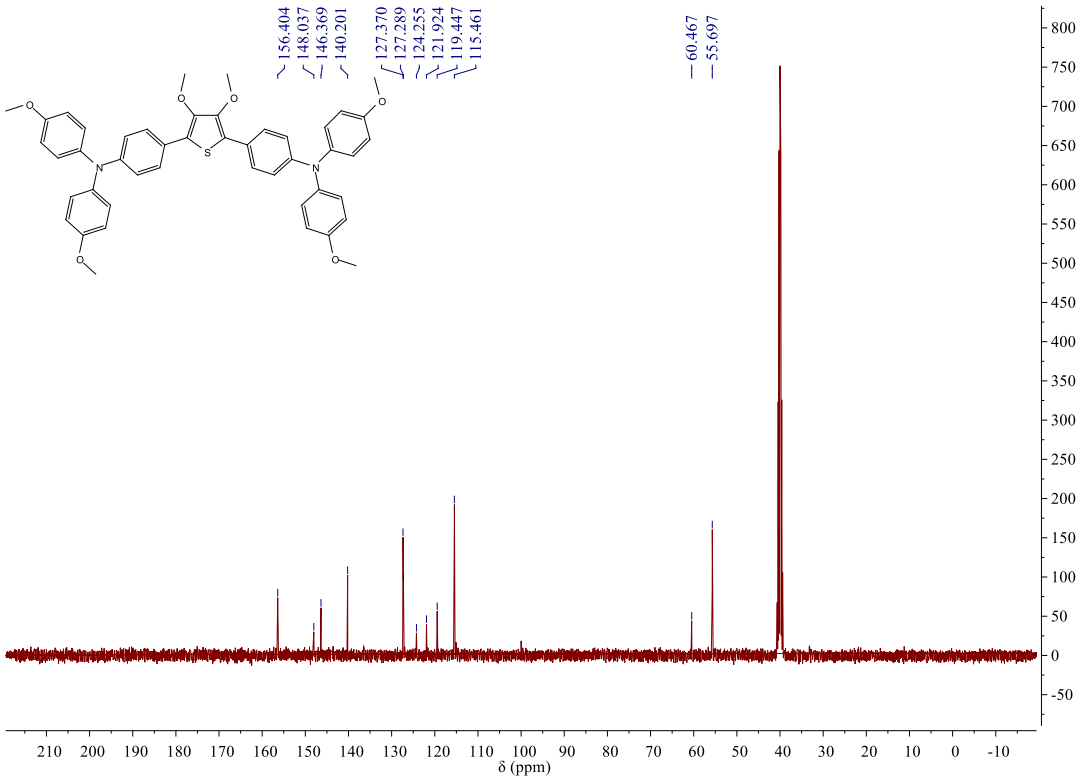

Figure S2. ^{13}C NMR spectrum of Z25

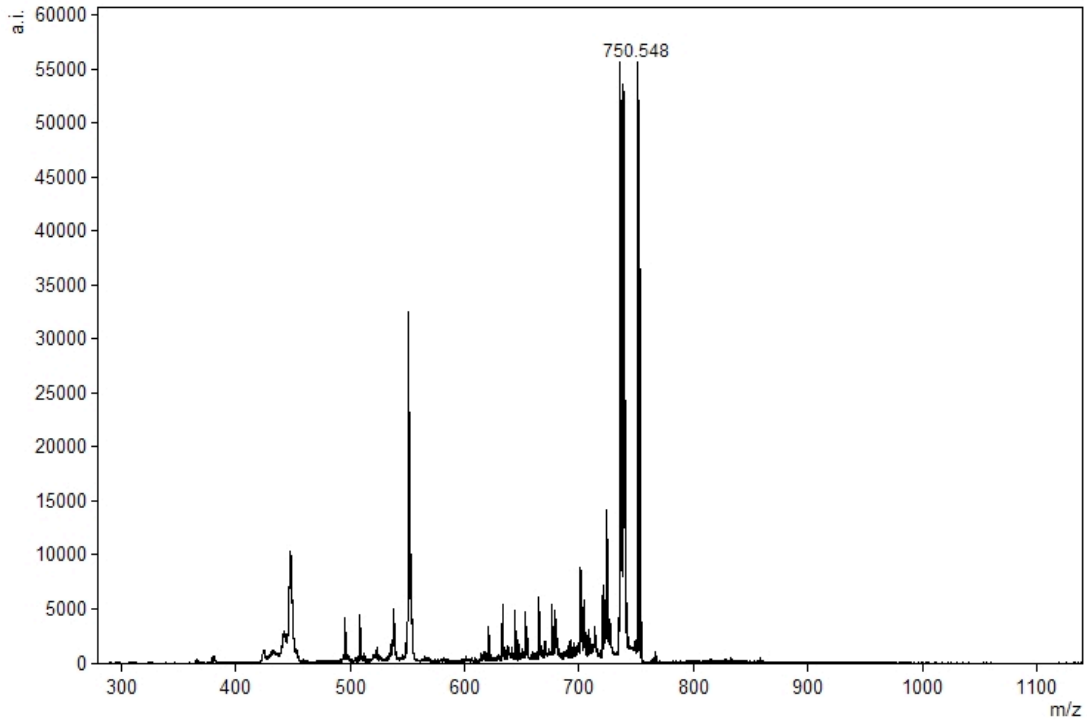

Figure S3.MALDI-TOF mass spectrum of Z25

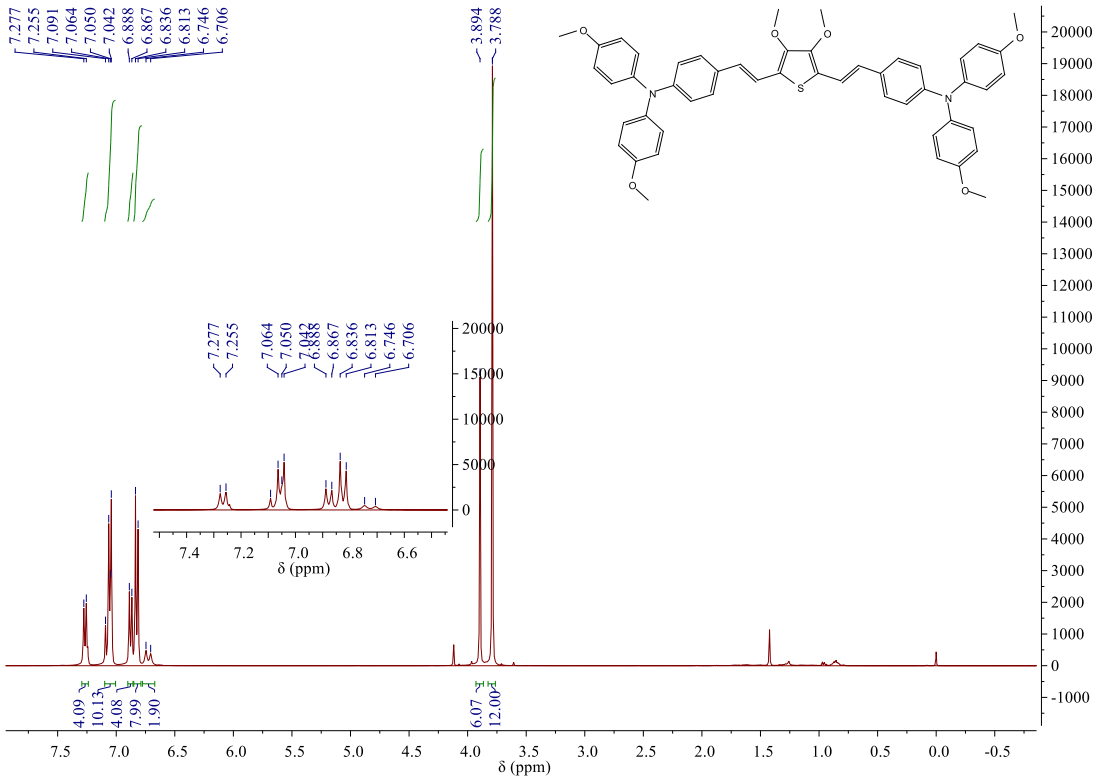

Figure S4. ^{1}H NMR spectrum of Z26

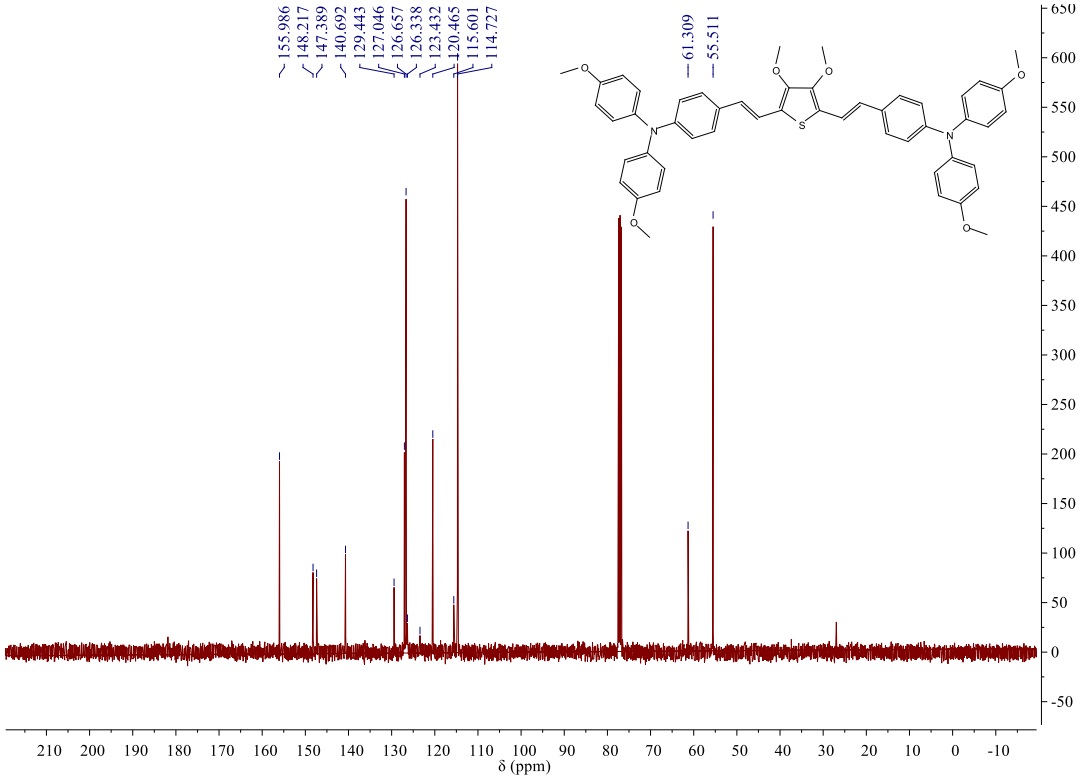

Figure S5. ^{13}C NMR spectrum of Z26

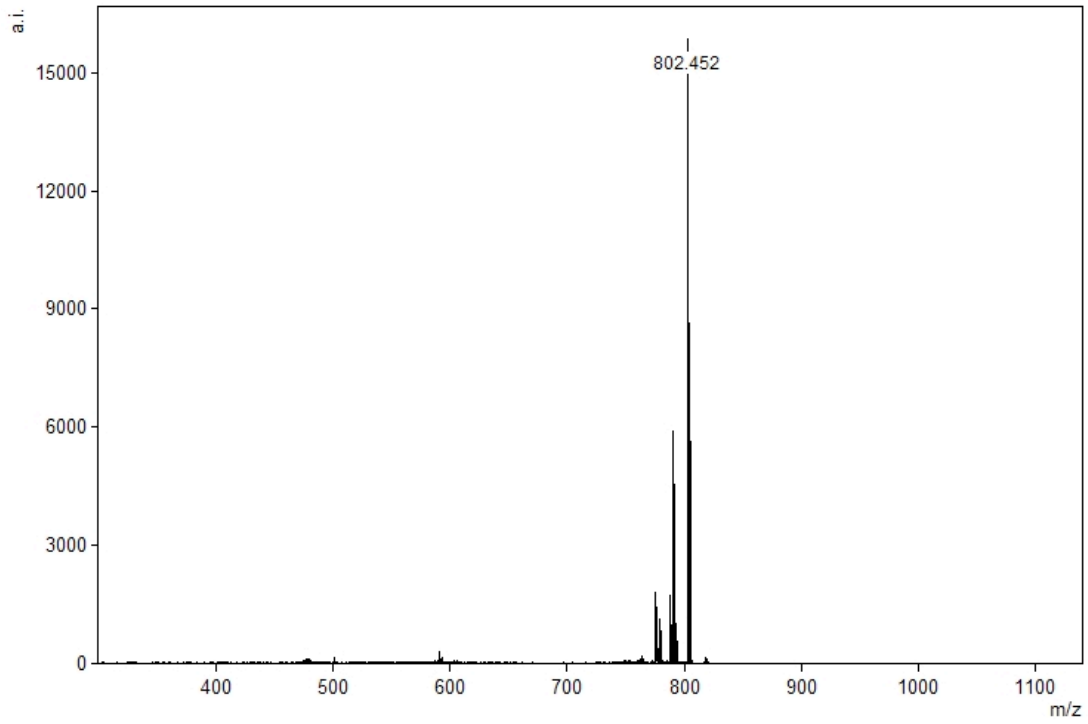

Figure S6.MALDI-TOF mass spectrum of Z26

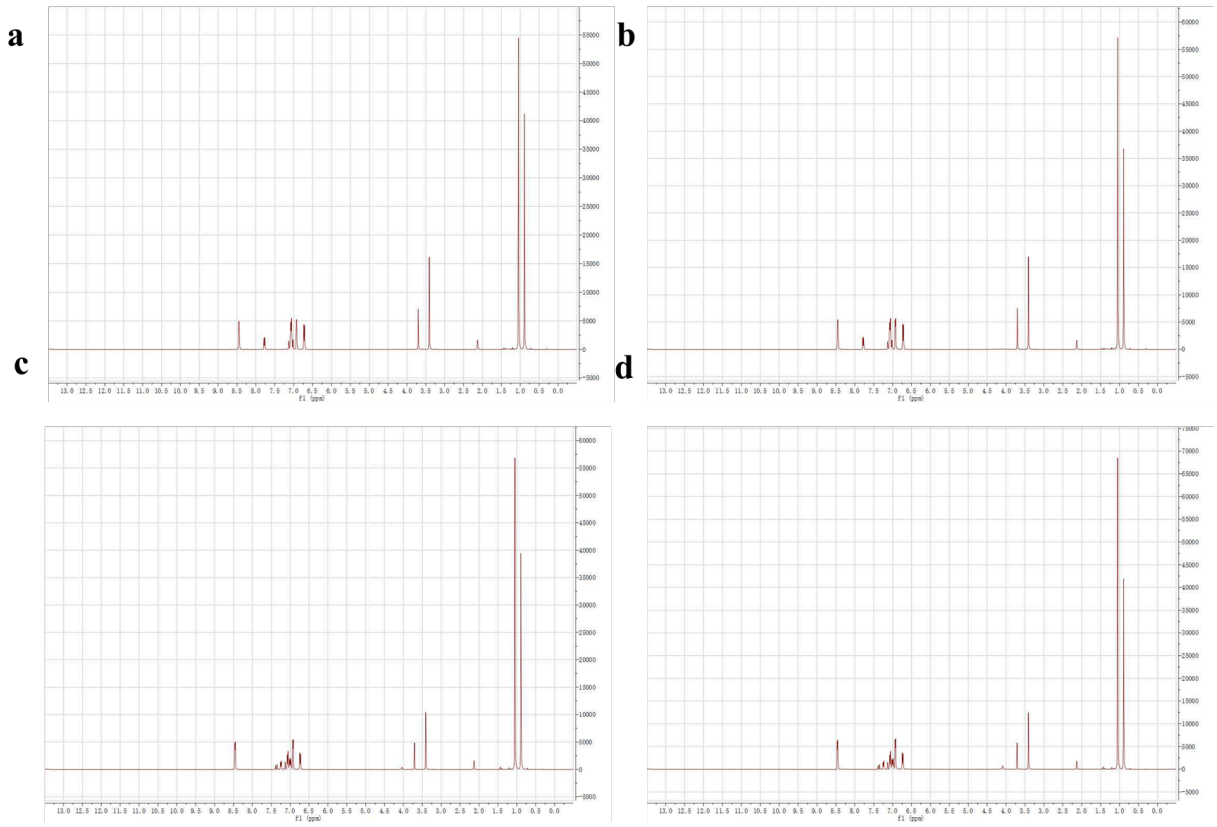

Figure S7. ^{1}H NMR spectrum in Deuterated toluene of (a)fresh Z25with additives; (b)Z25 with additives after 8 days;(c)fresh Z26 with additives;(d) Z26 with additives after 8 days

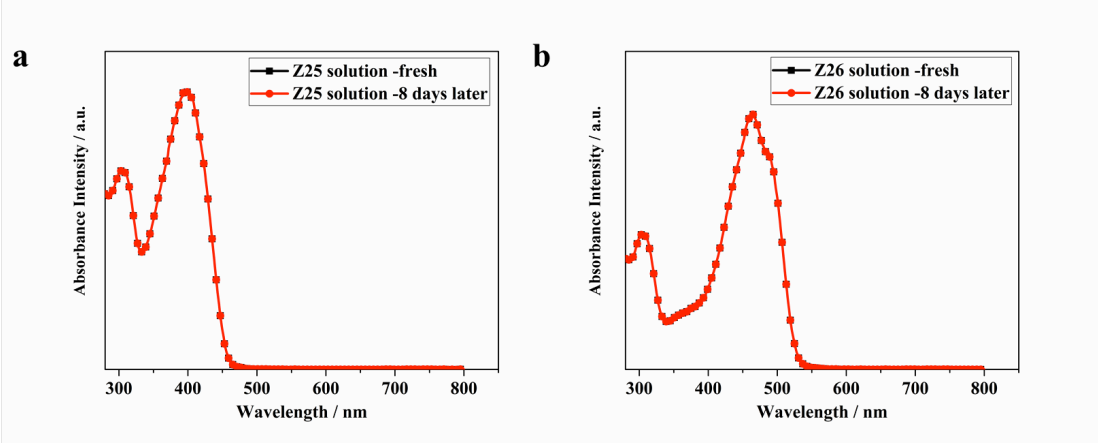

Figure S8. UV-Vis absorption spectra of the HTMs in CB solution with with additives (a)fresh Z25 and after 8 days;(b)fresh Z26 and after 8 days.

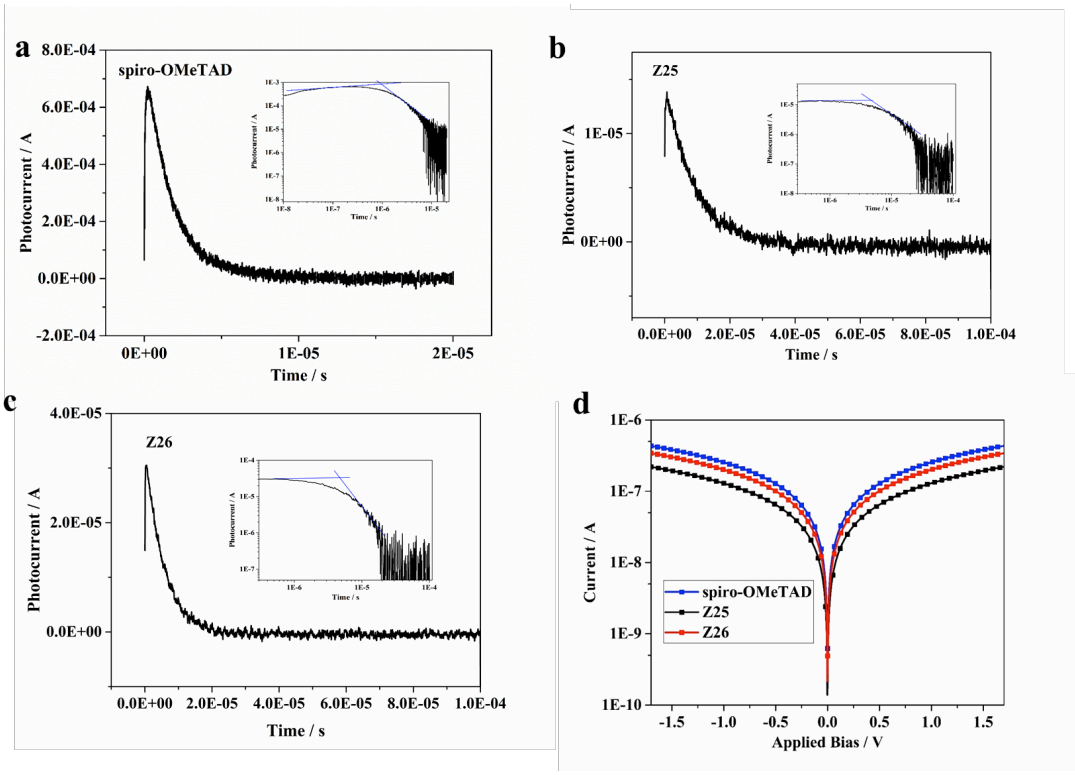

Figure S9 (a-c) TOF transients for different HTMs at room temperature; (d) Current–voltage characteristics of doped Z25, Z26 and *spiro*-OMeTAD based films

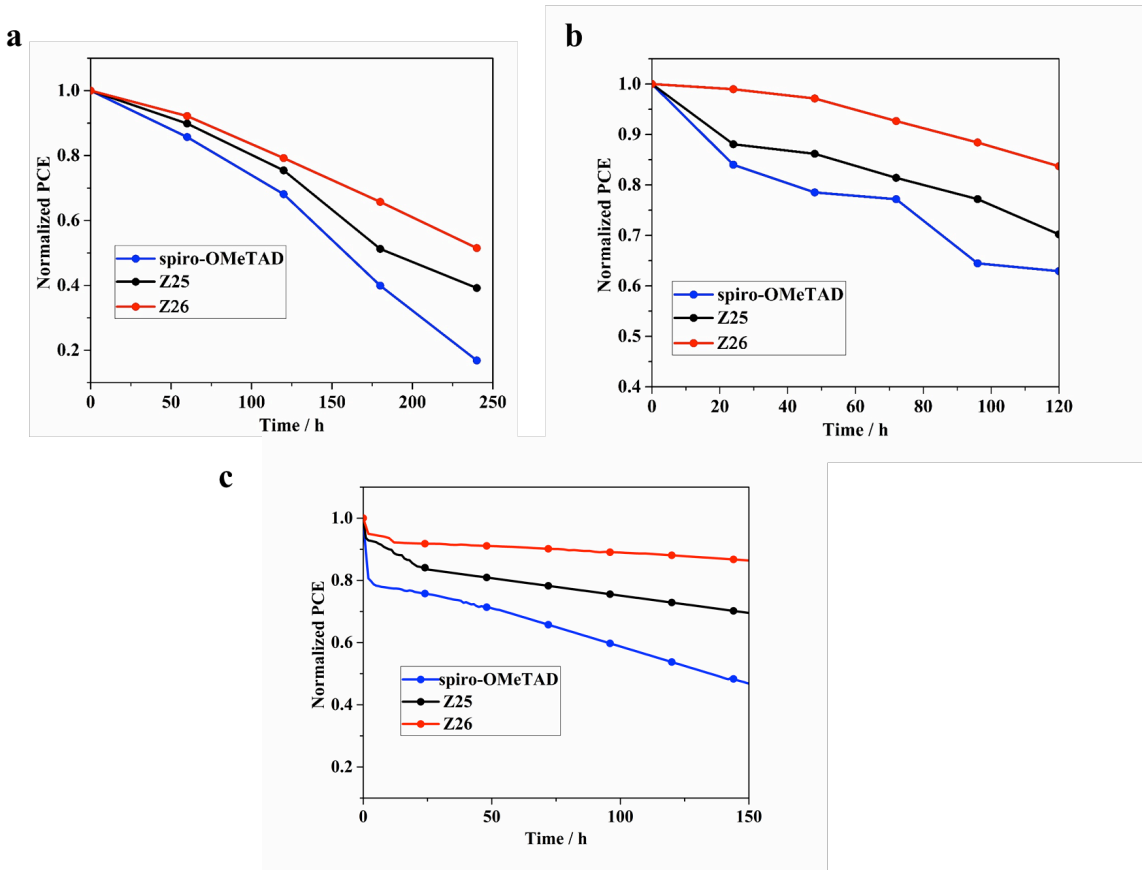

Figure S10 The stability of corresponding perovskite solar cells (a) in ambient environment of 85% relatively humidity under dark without any encapsulation at room temperature (b) in ambient environment of 40% relatively humidity under dark without encapsulation at 65℃;(c) under continuous full sun illumination at maximum power point tracking in ambient environment of 40% relatively humidity with encapsulation at room temperature.

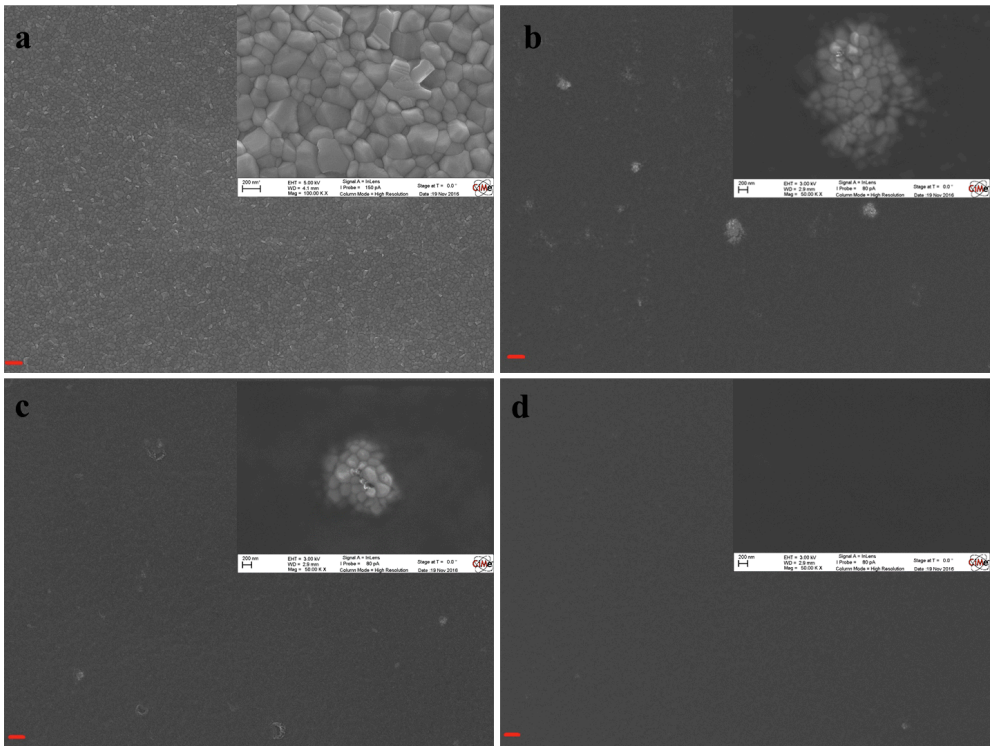

Figure S11 Surface view SEM images of (a) pristine perovskite ; (b) perovskite /spiro-OMeTAD;(c) perovskite /Z25; (d) perovskite /Z26. Scale bar is 2μm.

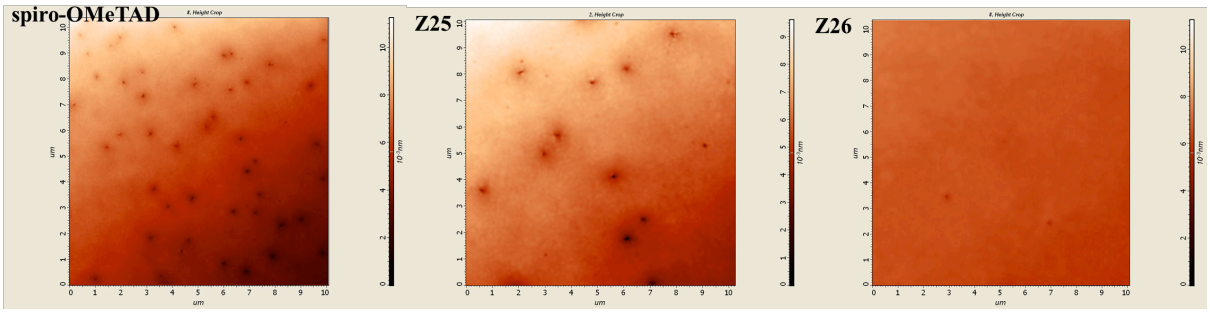

Figure S12 AFM images of different HTMs on perovskite film

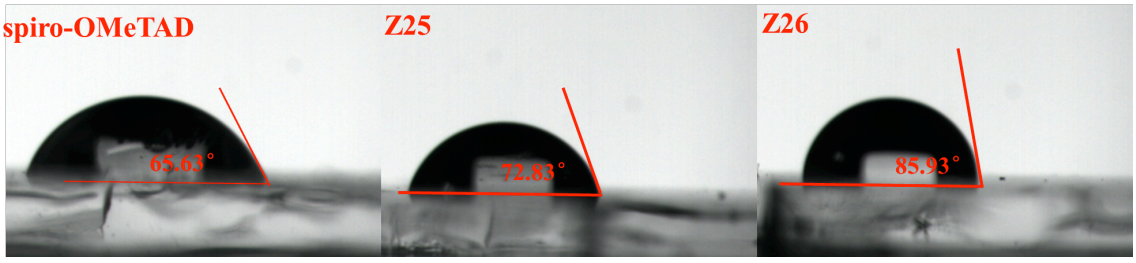

Figure S13 the contact angles between HTMs and water

Table S1 Reorganization energies of Z25 and Z26

HTM	E* (a.u)	E (a.u)	E+ * (a.u)	E+ (a.u)	λ1 (eV)	λ2(eV)	λ(eV)
D2	-2737.13337452	-2737.13832966	-2736.94679586	-2736.95141038	0.12556108 9209777	0.13482935 940599	0.26039044 8615767
D3	-2891.9454601	-2891.94891021	-2891.76939317	-2891.77255103	0.08592974 70010	0.09388221 700745	0.17981196 400845

Synthesis cost estimation of 1 gram HTMs

We roughly estimated the synthesis cost of 1 gram Z25 and Z26 according to the cost model that was described by Pablo *et al*.[1] and Osedach *et al*.[2] The price of raw materials are from http://www.sigmaaldrich.com/china-mainland.html .The estimated synthesis cost of Z25 and Z26 is 21.27 $/g and 21.13 $/g.Since these tables do not take into account several important parameters (e.g. energy consumption, waste treatment and labor), it was multiplied by a factor of 1.5[3] to get a more realistic estimation of lab synthesis costs of 31.91$/g and 31.70$/g (21.27 x 1.5 = 31.91$/g, 21.13x 1.5 = 31.70 $/g), which is much cheaper than that of *spiro*-OMeTAD(598.16 $/g).

For comparation ,we also caculate the cost of the more potential doped HTMs reported recently(PCE>19%). The cost of X59[4], DODF[5], IDIDF[6],FDT[3] and V862[7] multiplied by a factor of 1.5 are 118.89 $/g (79.26x 1.5 = 118.89 $/g), 807.21$/g (538.14 x 1.5=807.21$/g), 393.06$/g (262.04 x 1.5=393.06$/g), 58.30$/g[3] and 34.67$/g (23.11x 1.5 = 34.67$/g), respectively.The cost of tert-butylpyridine, Li-TFSI and FK209 are 7.59$/g, 11.26$/g and 78.64$/g,respectively.When considering the cost of dopants,the cost of **Z25, Z26, X59, DODF, IDIDF , FDT** and **V862** are **42.28$/g** (31.91+0.64 x 7.59+0.21x11.26+0.040 x 78.64 = 38.26$/g), **41.33$/g** (31.70+0.60 x 7.59+0.20x11.26+0.036 x 78.64 = 41.33$/g), **128.52$/g** (118.89+0.60 x 7.59+0.20x11.26+0.037 x 78.64 = 128.52$/g), **812.18$/g** (807.21+0.32 x 7.59+0.10x11.26+0.018 x 78.64 = 812.18$/g), **396.89$/g** (393.06+0.327 x 7.59+0.12x11.26 = 396.89$/g), **67.81$/g** (58.30+0.60 x 7.59+0.21x11.26+0.038 x 78.64 = 67.81$/g) and **40.29$/g** (34.67+0.38 x 7.59+0.11x11.26+0.019 x 78.64 = 40.29$/g).

In addition,we also caculated the cost of some dopant-free HTMs for comparation.such as Trux-OMeTAD[8], DORDTS-DFBT[9], DORDTS-TBDT[9],pBBTa-BDT2[10]and RCP[11]. The cost of these materials multiplied by a factor of 1.5 are **214.98 $/g** (143.32x 1.5 = 214.98 $/g), **1029.08$/g** (686.05 x 1.5=1029.08$/g), **775.91$/g** (517.27 x 1.5=775.91$/g), **491.03$/g** (327.35 x 1.5=491.03$/g) and **1193.24$/g** (795.49x 1.5 = 1193.24$/g), respectively.

The similar structure of Z25 is H101[12],H111[13] and H112[13].We also caculate their cost which are 254.84$/g , 167.54$/g and 170.28$/g (169.89 x 1.5 = 254.84$/g, 111.69x 1.5 = 167.54 $/g and 113.52x 1.5 = 170.28 $/g). When considering the cost of dopants,the cost of H101,H111 and H112 are **264.59$/g** (254.84+0.59 x 7.59+0.21x11.26+0.037 x 78.64 =

264.59$/g), **177.03$/g** (167.54+0.58x7.59+0.20x11.26+0.036 x 78.64 = 177.03$/g) and **179.58$/g** (170.28+0.57 x 7.59+0.19x11.26+0.036 x 78.64 = 179.58$/g)

Table S2 Materials quantities and cost for the synthesis of 1 gram Z25

Chemical name	Price of Chemical/$	Weight or amount reagent	Material cost /$
3,4-Dimethoxythiophene	79.83/25g	1.12g	3.58
Aniline	6.09/500mL	2mL	0.02
methylbenzene	2.90/500mL	15mL	0.09
N-bromobutanimide	5.22/100g	3.1g	0.16
1-Iodo-4-methoxybenzene	17.85/25g	0.78g	0.56
Copper(I) chloride	20.29/100g	0.13g	0.03
1,10-phenanthroline	3.34/5g	1.2g	0.80
xylene	4.21/500mL	18mL	0.15
Potassium hydroxide	3.77/500g	4.6g	0.03
N,N-Dimethylformamide	8.70/100mL	32mL	2.78
Sodium borohydride	5.8/100g	1.5g	0.09
dichloromethane	3.19/500 mL	200mL	1.28
Iodine	28.88/50g	1.8g	1.04
Tetrakis(triphenylphosphine) platinum(0)	5.89/1g	0.2g	1.18
Petroleum ether	4.20/500 mL	900mL	1.69
magnesium sulphate	1.50/500g	10g	0.03
Ethanol	3.33/500 mL	150mL	1.0
Silica gel (300-400mesh)	13.52/1kg	0.5kg	6.76
Total			21.27

Table S3 Materials quantities and cost for the synthesis of 1 gram Z26

Chemical name	Price of Chemical/$	Weight or amount reagent	Material cost /$
3,4-Dimethoxythiophene	79.83/25g	1.12g	3.58
Imidazole	5.08/100g	1.06g	0.05
Trifluoroacetic anhydride	11.76/25g	4.5mL	2.12
Acetonitrile	6.10/500mL	15mL	0.18
Hydrochloric acid	1.74/500mL	30mL	0.10
Aniline	6.09/500mL	2mL	0.02
1-Iodo-4-methoxybenzene	17.85/25g	0.78g	0.56

Copper(I) chloride	20.29/100g	0.13g	0.03
1,10-phenanthroline	3.34/5g	1.2g	0.80
xylene	4.21/500mL	18mL	0.15
Potassium hydroxide	3.77/500g	4.6g	0.03
phosphorus oxychloride	11.61/250g	1.2mL	0.06
N,N-Dimethylformamide	8.70/100mL	32mL	0.20
Sodium borohydride	5.8/100g	1.5g	0.09
Triethyl phosphite	8.56/100mL	2.1mL	0.18
dichloromethane	3.19/500 mL	200mL	1.28
Iodine	28.88/50g	1.8g	1.04
Tetrakis(triphenylphosphine) platinum(0)	5.89/1g	0.2g	1.18
Petroleum ether	0.94/500mL	900mL	1.69
magnesium sulphate	1.50/500g	10g	0.03
Ethanol	3.33/500 mL	150mL	1.00
Silica gel (300-400mesh)	13.52/1kg	0.5kg	6.76
Total			21.13

Table S4 Materials quantities and cost for the synthesis of 1 gram X59[4]

Chemical name	Price of Chemical/$	Weight or amount reagent	Material cost /$
NaOt-Bu	7.10/25g	0.92g	0.26
toluene	2.90/500 mL	30 mL	0.17
$P(t\text{-}Bu)_3$	26.23/0.25g	0.012g	1.26
$Pd(OAc)_2$	110.87/1g	0.014g	1.55
di(4-methoxylphenyl) amine	53.77/1g	0.76g	40.86
$MgSO_4$	1.50/500g	22g	0.06
petroleumether	4.20/500 mL	1200 mL	10.09
ethylacetate	5.36/500 mL	300 mL	3.22
phenol	126.79/25 mL	1.58 mL	8.01
2,7-dibromo-9-fluor-enone	48.99/25g	0.57g	1.12
Methane sulfonic acid	11.36/100g	0.64g	0.07
methaol	3.91/500 mL	780 mL	6.10
silica gel	13.52/1kg	0.5kg	6.76
Total			79.26

Table S5 Materials quantities and cost for the synthesis of 1 gram DODF[5]

Chemical name	Price of	Weight or amount	Material cost

	Chemical/$	reagent	/$
methaol	3.91/500 mL	200 mL	1.57
THF	7.25/500 mL	50 mL	0.72
$MgSO_4$	1.45/500g	12g	0.03
$Pd_2(dba)_3$	123.62/1g	0.17g	21.02
toluene	2.90/500 mL	47.6 mL	0.28
NaOt-Bu	7.10/25g	0.67g	0.19
di(4-methoxylphenyl) amine	53.77/1g	1.33g	71.51
dichloromethane	3.19/500 mL	500 mL	3.19
acetic acid	2.90/500 mL	68 mL	0.39
2,7-dibromo-9-fluor-enone	48.99/25g	2.48g	4.86
n-BuLi	33.62/100 mL	2.45 mL	0.82
hexane	7.54/500 mL	600 mL	9.04
trimethylsilyl chloride	277.39/1g	0.98g	271.84
lithium diisopropylamide	91.11/75g	3.85g	4.68
3,3'-dibromo-2,2'-bithiophene	106.14/1g	1.13g	119.95
Xphos	125.14/1g	0.17g	21.27
silica gel	13.52/1kg	0.5kg	6.76
Total			538.14

Table S6 Materials quantities and cost for the synthesis of 1 gram IDIDF[6]

Chemical name	Price of Chemical/$	Weight or amount reagent	Material cost /$
$CHCl_3$	6.52/500 mL	200 mL	2.61
hexane	7.54/500 ml	760 mL	11.46
$MgSO_4$	7.54/500g	24g	0.07
dichloromethane	3.19/500 mL	580 mL	3.70
hydrochloric acid	5.94/500 mL	30 mL	0.36
NaOH	9.57/500g	5g	0.10
THF	7.25/500 mL	50 mL	0.72
tetrakis(triphenylphosphine) palladium(0)	67.14/1g	0.17g	11.42
5-hexyl-2,2-bithiophene-5-boronicacid pinacol ester	104.96/1g	1.19g	124.90
ethylacetate	5.36/500 mL	300 mL	3.22
1-bromohexane	45.36/1g	1.31g	59.42
NaH	4.20/100g	0.19g	0.01
AcOH	3.04/500 mL	600 mL	3.65
stannous chloride	21.16/10g	9.53g	20.16
acetic acid	2.90/500 mL	9.62 mL	0.06
$NaHSO_3$	3.19/500g	20g	0.13
Adogen 464	15.65/25g	1.41g	0.88
triethylamine	5.21/500 mL	8 mL	0.08

copper(I) iodide	20.29/100g	0.13g	0.03
bis(triphenylphosphine)palladium(II) dichloride	56.52/5g	0.23g	2.60
acetone	5.96/500 mL	50 mL	0.70
18-crown-6	16.96/25g	0.24g	0.16
K_2CO_3	6.38/500g	1.28g	0.02
trimethylsilylacetylene	24.64/25g	1.13g	1.11
$Na_2S_2O_3$	3.19/500g	12g	0.08
$NaHCO_3$	36.52/250g	15g	2.19
KI	6.38/25g	6.78g	1.73
$NaNO_2$	4.20/500g	6.46g	0.05
H_2SO_4	1.88/500 mL	11.98 mL	0.05
N-bromosuccinimide	5.22/100g	2.84g	0.15
5-Fluoro-2-nitrobenzene	21.59/5g	2.37g	10.24
			262.04

Table S7 Materials quantities and cost for the synthesis of 1 gram Trux-OMeTAD [8]

Chemical name	Price of Chemical/$	Weight or amount reagent	Material cost /$
1-Indanone	8.40/5g	0.6g	1.01
hydrochloric acid	5.94/500 mL	3 mL	0.04
acetic acid	2.90/500 mL	2 mL	0.01
THF	7.25/500 mL	20 mL	0.29
n-BuLi	33.63/100 mL	6.48 mL	2.18
1-bromohexene	38.84/500 mL	1.74 mL	0.14
$FeCl_3$	7.10/100g	0.018g	0.00
$CHCl_3$	6.52/500g	5.4g	0.07
Br_2	5.65/25 mL	0.18 mL	0.04
di(4-methoxylphenyl) amine	53.77/1g	0.81g	43.55
$Pd_2(dba)_3$	123.62/1g	0.027g	3.34
$P(t\text{-}Bu)_3$	26.23/0.25g	0.06g	6.30
NaOt-Bu	7.10/25g	0.92g	0.26
toluene	2.89/500 mL	20 mL	0.12
acetone	6.96/500 mL	40 mL	0.56
dichloromethane	15.51/500 mL	600 mL	18.61
NH_4Cl	33.04/500g	12g	0.79
$MgSO_4$	1.45/500g	24g	0.07
silica gel	10.87/1000g	2100g	22.83
ethanol	3.33/500 mL	400 mL	2.67
hexane	7.53/500 mL	2000 mL	30.14
ethyl acetate	12.90/500 mL	400 mL	10.32

Total			143.32

Table S8 Materials quantities and cost for the synthesis of 1 gram DORDTS-DFBT [9]

Chemical name	Price of Chemical/$	Weight or amount reagent	Material cost /$
4*H*-Silolo[3, 2-*b*:4, 5-*b*'] dithiophene	246.28/1g	1.67g	411.45
4,7-Dibromo-5,6-difluoro-2,1,3-benzothiadiazole	48.41/0.25g	0.65g	125.86
n-BuLi	33.62/100ml	2.3g	0.77
$POCl_3$	8.40/25 mL	2.35 mL	0.79
DMF	8.70/100 mL	20.09 mL	1.75
N-Bromosuccinimide	10.00/100g	2.4g	0.24
$Pd(PPh_3)_4$	44.93/0.1g	0.086g	38.64
triethylamine	9.57/500 mL	1.2 mL	0.02
3-octyl-rodanine	18.99/0.5g	1.47g	55.82
Me_3SnCl	53.04/5g	1.1g	11.67
dichloromethane	15.50/500 mL	300 mL	9.30
Na_2SO_4	7.25/500g	22g	0.32
hexane	7.54/500 mL	1000 mL	15.07
toluene	2.90/500 mL	172.2 mL	1.00
silica gel	10.87/1000g	900g	9.78
chloroform	6.52/500 mL	176.4 mL	2.30
1,2-dichloroethane	7.39/500 mL	86.2 mL	1.27
Total			686.05

Table S9 Materials quantities and cost for the synthesis of 1 gram DORDTS-TBDT [9]

Chemical name	Price of Chemical/$	Weight or amount reagent	Material cost /$
4*H*-Silolo[3, 2-*b*:4, 5-*b*'] dithiophene	246.28/1g	1.27g	312.90
n-BuLi	33.62/100 mL	1.5 mL	0.50
$POCl_3$	8.40/25 mL	2.12 mL	0.71
DMF	8.70/100 mL	30 mL	2.61
N-Bromosuccinimide	10.00/100g	0.63g	0.06
$Pd(PPh_3)_4$	44.93/0.1g	0.16g	71.88
triethylamine	9.57/500 mL	1.2 mL	0.02
3-octyl-rodanine	18.99/0.5g	1.75g	66.45
Me_3SnCl	53.04/5g	1.5g	15.91
dichloromethane	15.50/500 mL	400 mL	12.41
Na_2SO_4	7.25/500g	22g	0.33
hexane	7.54/500 mL	1100 mL	16.58
toluene	2.90/500 mL	125.2 mL	0.73

silica gel	10.87/1000g	1300g	14.13
chloroform	6.52/500 mL	156.5 mL	2.04
Total			517.27

Table S10 Materials quantities and cost for the synthesis of 1 gram pBBTa-BDT2 [10]

Chemical name	Price of Chemical/$	Weight or amount reagent	Material cost /$
4-bromophenol	15.79/25g	1.03g	0.65
potassium carbonate	8.55/500g	3.64g	0.06
DMF	8.70100 mL	21 mL	1.83
2-hexyldecyl bromide	28.70/5g	1.81	10.39
diethyl ether	72.4640 mL	45 mL	81.52
NaCl	7.97500g	12g	0.19
MgSO4	1.45/500	23g	0.07
Mg	1.74/25g	0.397g	0.03
THF	7.25/500 mL	40 mL	0.58
benzo[1,2-b:4,5-b′]dithiophene-4,8-dione	128.11/1g	0.3g	38.43
$SnCl_2$	7.39/500g	6.54g	0.10
hexane	7.54/500 mL	1200 mL	18.09
dichloromethane	15.51/500 mL	600 mL	18.61
n-BuLi	33.62/100 mL	0.77 mL	0.26
Trimethyltin chloride	53.04/5g	2.04g	21.64
(BrTh)2-BBTa	318.84/1g	0.384g	122.43
Pd(PPh3)4	44.93/0.1g	0.027g	12.13
toluene	2.90/500 mL	60 mL	0.35
Total			327.35

Table S11 Materials quantities and cost for the synthesis of 1 gram RCP [11]

Chemical name	Price of Chemical/$	Weight or amount reagent	Material cost /$
2,6-bis(trimethyltin)-4,8-bis(2-ethylhexyl-2-thenyl)-benzo[1,2-b:4,5-b′]dithiophene	67.39/0.1g	0.60g	404.35
4,7-bis(5-bromo-4-dodecylthiophen-2-yl)-2,1,3-benzothiadiazole	161.96/0.2g	0.26g	213.78
4,7-bis(5-bromothiophen-2-yl)-5,6-bis(dodecyloxy)benzo[c][1,2,5] thiadiazole	507.24/1g	0.27g	139.09
tris(dibenzylideneacetone) dipalladium	28.70/1g	0.64g	18.42
tri(o-tolyl)phosphine	7.39/1g	0.80g	5.94
chlorobenzene	9.42/500 mL	9.00 mL	0.17
2-tributylstannylthiophene	92.75/10g	0.03g	0.28

2-bromothiophene	14.92/10g	0.19g	0.29
methanol	7.39/500 mL	60.00 mL	0.89
acetone	6.96/500 mL	138.00 mL	1.92
hexane	7.54/500 mL	480.00 mL	7.23
chloroform	6.52/500 mL	240.00 mL	3.13
Total			795.49

Table S12 Materials quantities and cost for the synthesis of 1 gram H101 [12]

Chemical name	Price of Chemical/$	Weight or amount reagent	Material cost /$
silica gel	13.52/1kg	1560g	21.09
$MgSO_4$	1.45/500g	25g	0.07
$Pd(PPh_3)_4$	44.39/0.1g	0.09g	40.43
K_2CO_3	6.38/500g	3.85g	0.05
THF	7.25/500mL	40mL	0.58
Methoxybenzene	89.36/5mL	4.75mL	84.89
KI	6.38/25g	7.6g	1.94
CH_3OH	3.91/500mL	76mL	0.59
H_2SO_4	1.88/500mL	3.61mL	0.01
H_2O_2	3.62/500mL	9.5mL	0.07
CH_2Cl_2	3.19/500mL	101mL	0.64
Na_2SO_4	7.25/500g	33g	0.48
ethyl acetate	5.36/500mL	200mL	2.14
petroleum ether	4.20/500mL	1600mL	13.45
aniline	6.09/500mL	0.78mL	0.01
1,10-phenanthroline	3.33/5g	0.31g	0.21
toluene	2.90/500mL	27.2mL	0.16
CuCl	7.79/100g	0.17g	0.01
KOH	3.77/500g	3.81g	0.03
acetic acid	2.90/500mL	2.31mL	0.01
NBS	5.22/100g	6.9g	0.36
CCl_4	2.17/500mL	22.4mL	0.10
n-BuLi	33.62/100mL	4.05mL	1.36
trimethyl borate	4.46/25mL	0.69mL	0.13
HCl	5.94/500mL	6mL	0.07
3,4-ethylenedioxythiophene	21.59/5g	0.23g	0.99
Total			169.89

Table S13 Materials quantities and cost for the synthesis of 1 gram H111 [13]

Chemical name	Price of Chemical/$	Weight or amount reagent	Material cost /$
KI	6.38/25g	6.4g	1.63
CH_3OH	3.91/500mL	64mL	0.50
H_2SO_4	1.88/500mL	3.05mL	0.01

H_2O_2	3.62/500mL	7.82mL	0.06
CH_2Cl_2	3.19/500mL	101mL	0.64
Na_2SO_4	7.25/500g	33g	0.48
ethyl acetate	5.36/500mL	200mL	2.14
petroleum ether	4.20/500mL	1600mL	13.45
aniline	6.09/500mL	0.87mL	0.01
1,10-phenanthroline	3.33/5g	0.34g	0.23
toluene	2.90/500mL	30.4mL	0.18
CuCl	7.79/100g	0.19g	0.02
KOH	3.77/500g	4.26g	0.03
acetic acid	2.90/500mL	2.58mL	0.01
NBS	5.22/100g	7.2g	0.38
CCl_4	2.17/500mL	24.8mL	0.11
n-BuLi	33.62/100mL	4.4mL	1.48
trimethyl borate	4.46/25mL	0.75mL	0.14
HCl	5.94/500mL	1.5mL	0.02
Tetrabromothiophene	168.00/5g	0.42g	14.11
K_2CO_3	6.38/500g	10.4g	0.13
$Pd0(PPh_3)_4$	44.39/0.1g	0.12g	53.91
THF	7.25/500mL	45.6mL	0.66
silica gel	13.52/1kg	1580g	21.36
Total			111.69

Table S14 Materials quantities and cost for the synthesis of 1 gram H112 [13]

Chemical name	Price of Chemical/$	Weight or amount reagent	Material cost /$
KI	6.38/25g	5.44g	1.39
CH_3OH	3.91/500mL	54.4mL	0.43
H_2SO_4	1.88/500mL	2.58 mL	0.01
H_2O_2	3.62/500mL	6.79 mL	0.05
CH_2Cl_2	3.19/500mL	101 mL	0.64
Na_2SO_4	7.25/500g	33g	0.48
ethyl acetate	5.36/500mL	300 mL	3.22
petroleum ether	4.20/500mL	1800 mL	15.13
aniline	6.09/500mL	0.75 mL	0.01
1,10-phenanthroline	3.33/5g	0.3g	0.20
toluene	2.90/500mL	18.06 mL	0.10
CuCl	7.79/100g	0.16g	0.01
KOH	3.77/500g	3.7g	0.03
acetic acid	2.90/500mL	2.24 mL	0.01
NBS	5.22/100g	0.57g	0.03
CCl_4	2.17/500mL	21.71 mL	0.09
n-BuLi	33.62/100mL	3.87 mL	1.30
trimethyl borate	4.46/25mL	0.66 mL	0.12
HCl	5.94/500mL	1.3 mL	0.02

K_2CO_3	6.38/500g	11.2g	0.14
$Pd0(PPh_3)_4$	44.39/0.1g	0.14g	62.90
THF	7.25/500mL	45.6 mL	0.66
silica gel	13.52/1kg	1680g	22.71
$AgNO_3$	11.59/5g	0.68g	1.58
potassium fluoride	1.23/25g	0.23g	0.01
DMSO	14.20/500mL	27.6 mL	0.78
$PdCl_2(PhCN)_2$	28.70/1g	0.02g	0.57
2,3-dibromothiophene	20.00/5g	0.22g	0.88
Total			113.52

Table S15 The compare of different HTMs

HTMs	Structure	T_g (°C)	PCE (%)	Hole mobility	Long-term stability	Perovskite	Cost
Trux-OMeTAD	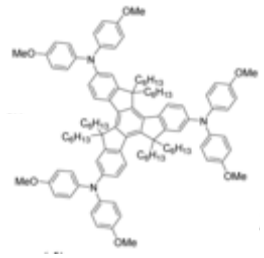	n/a	18.6	2.3×10^{-3} $cm^2V^{-1}s^{-1}$	n/a	$CH_3NH_3PbI_3$	214.98 \$/g
DORD TS-TBDT	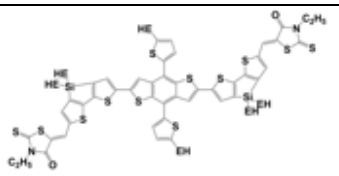	n/a	16.2	1.0×10^{-4} $cm^2V^{-1}s^{-1}$	PCE drooped by 5% after 220 hours without encapsulation in the N_2 glove box	$CH_3NH_3PbI_{3-X}Cl_X$	775.91 \$/g
DORD TS-DFBT	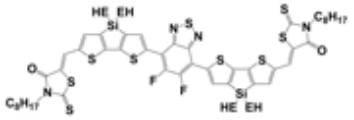	n/a	6.2	2.4×10^{-6} $cm^2V^{-1}s^{-1}$	PCE drooped by 80% after 220 hours without encapsulation in the N_2 glove box	$CH_3NH_3PbI_{3-X}Cl_X$	1029.08 \$/g
RCP	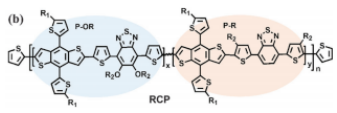	n/a	17.3	3.34×10^{-3} $cm^2V^{-1}s^{-1}$	At 25% or 75% humidity, the efficiency of the RCP device was nearly constant over 1400 h.	$CH_3NH_3PbI_3$	1193.24\$/g
pBBTa-BDT**2**	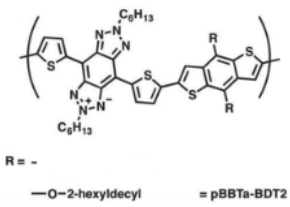	n/a	12.3	2.0×10^{-3} $cm^2V^{-1}s^{-1}$	pBBTa-BDT2-based solar cells exhibit stable PCE over 500 h	$CH_3NH_3PbI_{3-X}Cl_X$	491.03 \$/g

HTMs	Structure	T_g (°C)	PCE (%)	Hole mobility	Long-term stability	Perovskite	Cost
FDT	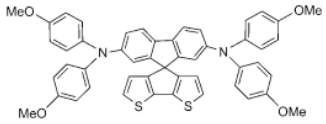	110	20.2	n/a	n/a	$(FAI)(PbI_2)_{1.1}(MABr)_{0.2}(PbBr_2)_{0.2}$	67.81 $/g
V862	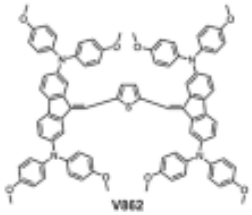	138	19.96	1.0×10^{-3} $cm^2V^{-1}s^{-1}$	under dry conditions in the dark for 50 days,there is some degree of degradation in the PSC devices constructed using V862	$(FAI)(PbI_2)_{1.1}(MABr)_{0.2}(PbBr_2)_{0.2}$	40.29 $/g
DDOF	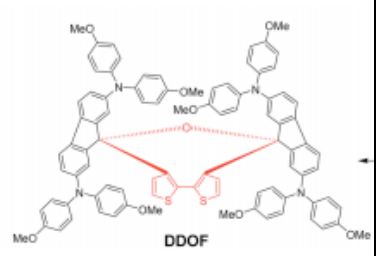	157	19.4	n/a	The cells with DDOFmaintained around 95% of their initial PCE at a relative humidity of 10% without any encapsulation for 1000 h. After250 h under a constant illumination, the initial MPO values for DDOF decay to 65%.	$(FAPbI_3)_{0.85}(MAPbBr_3)_{0.15}$	812.18 $/g
X59	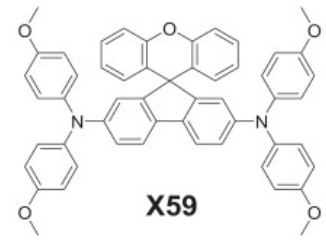	n/a	19.8	5.5×10^{-5} $cm^2V^{-1}s^{-1}$	Initial stability test of the X59 based PSCs suggest similar level of stability as that of the reported spiro-OMeTAD based devices	$(FAPbI_3)_{0.85}(MAPbBr_3)_{0.15}$	128.52 $/g
IDIDF	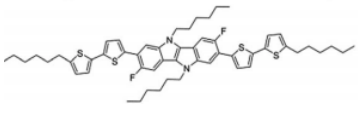	n/a	19.05	1.69×10^{-3} $cm^2V^{-1}s^{-1}$	The efficiency was maintained at almost 90% of its initial value after 50 hwithout encapsulation under a high humidity of 85%.	$(FAPbI_3)_{0.92}(MAPbBr_3)_{0.08}$	812.08 $/g
Z25	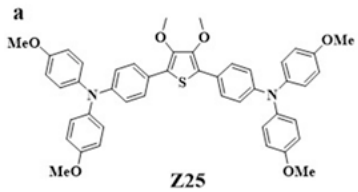	77	16.9	7.66×10^{-5} $cm^2\ V^{-1}\ s^{-1}$	PCE decreased to 66.8% of the initial value in the Z25-based perovskite based solar cells after 800 h. There is 42% drop after 300 h	$[(FAI)_{0.81}(PbI_2)_{0.85}(MABr)_{0.15}(PbBr_2)_{0.15}]$	42.28 $/g

					under continuous full sun illumination and maximum power point tracking for Z25 -based perovskite solar cell,		
Z26	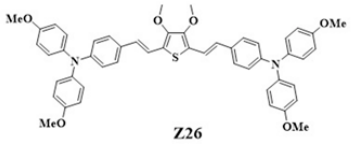 Z26	98	20.1	1.34×10^{-4} cm^2 V^{-1} s^{-1}	The PCE maintained 85.5% of the initial value in the Z26-based perovskite solar cell. There is 14% efficiency drop after 300 h under continuous full sun illumination and maximum power point tracking for Z26-based perovskite solar cell.	$[(FAI)_{0.81}(PbI_2)_{0.85}(MABr)_{0.15}(PbBr_2)_{0.15}]$	41.33 $/g
H101	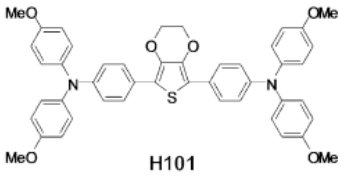 H101	73	13.2	n/a	spiro-OMeTAD and H101 have comparable thermal stability at 70℃ for 7 days.	$CH_3NH_3PbI_3$	264.59 $/g
H111	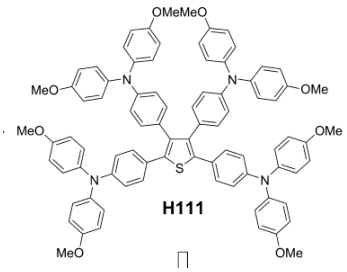 H111	100	15.4	n/a	The moderate decreases in performance by 16% for H111 -based devices	$CH_3NH_3PbI_3$	177.03 $/g
H112	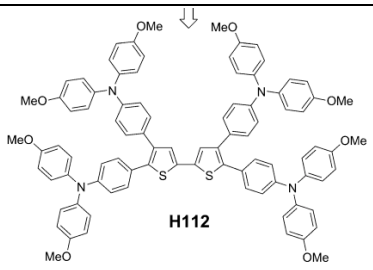 H112	120	15.2	n/a	The moderate decreases in performance by 16% for H112 -based devices	$CH_3NH_3PbI_3$	179.58 $/g

References

[1] M. L.Petrus, T. Bein, T. J.Dingemans, P.Docampo, J. Mater. Chem. A,2015, 3, 12159-12162.

[2] T. P. Osedach, T. L.Andrew, V.Bulovic, Energy Environ. Sci.,2013,6, 711-718.

[3] M.Saliba, S.Orlandi, T.Matsui, S.Aghazada, M.Cavazzini, J.Correa-Baena, P.Gao, R. Scopelliti, E.Mosconi, K.Dahmen, F.D.Angelis, A.Abate, A.Hagfeldt, G.Pozzi, M.Graetzel ,M.K.Nazeeruddin, Nature Energy, 2016,15017.

[4] D.Q. Bi, B. Xu, P. Gao, L.C. Sun, M.Grätzel,A.Hagfeldt, Nano Energy,2016, 23, ,138–144.

[5] K.Rakstys, S.Paek, M.Sohail, P.Gao, K.T.Cho, P.Gratia, Y.Lee, K.H.Dahmen, M.K.Nazeeruddin, J. Mater. Chem. A. 2016, 4, 18259-18264.

[6] I.Cho,N.J. Jeon,O.K. Kwon,D.W.Kim,E.H.Jung,J.H.Noh,J.W.Seo,S.I.Seok,S.Y.Park, Chem. Sci., 2017,8, 734-741.

[7]T.Malinauskas,M.Saliba,T.Matsui,M.Daskeviciene,S.Urnikaite,P.Gratia,R.Send,H.Won neberger,I.Bruder,M. Graetzel,V.Getautis,M.K. Nazeeruddin, Energy Environ. Sci., 2016, 9, 1681-1686.

[8]C.Y.Huang, W.F. Fu, C.Z.Li, Z.Q.Zhang, W.M.Qiu, M.M.Shi, P.Heremans, A.L Jen, H.Z.Chen, J. Am. Chem. Soc., 2016, 138 (8), 2528–2531

[9]Y.S. Liu, Z.R.Hong, Q.Chen, H.J.Chen, W.H.Chang, Y.Yang, T.B.Song, Y.Yang, Adv. Mater. 2016,28,440-446.

[10] H.C. Liao, T.L.D. Tam, P.J. Guo, Y.L.Wu, E.F. Manley, W.Huang, N.J. Zhou, C.M.M. Soe, B.H.Wang, M.R.Wasielewski, L.X. Chen, M.G.Kanatzidis, A.Facchetti, R. P. H. Chang, T.J. Marks, Adv. Energy Mater. 2016, 6, 1600502

[11] G.W. Kim, G. Kang, J.Kim, G.Y. Lee, H.I.Kim, L.Pyeon, J.Lee, T.Park, Energy Environ. Sci., 2016,9, 2326-2333.

[12] H.R. Li, K.W. Fu, A.Hagfeldt, M.Gratzel, S.G. Mhaisalkar, A.C. Grimsdale, Angew. Chem. Int. Ed. 2014, 53, 4085-4088

[13] H.R. Li, K.W. Fu,P. P. Boix, L. H. Wong,A.Hagfeldt, M. Gratzel, S. G. Mhaisalkar, A.C. Grimsdale, ChemSusChem, 2014, 7, 3420-3425.